Mapping suspended sediment concentrations using the diffuse attenuation coefficient (K_d) and multi spectral and spatiotemporal images in Caribbean coastal waters of Colombia

by

Pilar Lozano-Rivera

Thesis submitted to the International Institute for Geo-information Science and Earth Observation in partial fulfilment of the requirements for the degree of Master of Science in Geo-information Science and Earth Observation, Specialisation: Water resources and environmental management

Thesis Assessment Board

Chairman: Prof. Dr. Ing. Wouter Verhoef (ITC)
External Examiner: Dr. H.J. van der Woerd (VU-Amsterdam)
First Supervisor: Dr. Ir. Mhd. Suhyb Salama (ITC)
Second Supervisor: Dr. Ir. Chris M. Mannaerts (ITC)

INTERNATIONAL INSTITUTE FOR GEO-INFORMATION SCIENCE AND EARTH OBSERVATION
ENSCHEDE, THE NETHERLANDS

Disclaimer

This document describes work undertaken as part of a programme of study at the International Institute for Geo-information Science and Earth Observation. All views and opinions expressed therein remain the sole responsibility of the author, and do not necessarily represent those of the institute.

Abstract

Suspended sediments (SS) are an important determinant of water quality in coastal zones. High load of river-discharged sediments have been implicated in acute damage to coral reefs. SS reduce the light available to aquatic vegetation and provide substrate for transport of nutrients, heavy metals and pathogenic bacteria from rivers to coastal ecosystems. The study area of this research is the Caribbean Sea of Colombia, in the discharge zone of the Magdalena and Sinú rivers. This area includes one of Colombia's most important coral reef protected areas, Rosario and San Bernardo Islands. This region suffers from scarcity of reliable in-situ data on SS and water optical properties. There is very little remote sensing method that can be used to estimate SS and study their effects on aquatic ecosystem. Thus the aim of this research is to estimate SS concentration with a single optical model based on the diffuse attenuation coefficient (K_d), applied to multi-spectral (SeaWiFS and MODIS) spatio-temporal images (1998 - 2008). Ocean optics modelling is based on K_d using underwater optical measurements of downwelling irradiance (E_d) at two depths (50 and 100 cm) and *in situ* above-water leaving reflectance (L_W). *In situ* measurements of SS concentration and fluorescence were made at 11 sites. Coefficients were derived from a subset of these measurements to link ocean colour ratio to K_d for SS in turbid waters. This empirical model was validated with independent *in situ* measurements. The model successfully reproduces the measured K_d ($R^2 > 0.98$, mean relative error 1.1%). Multi sensors derived K_d were merged using error-weighted averaging (mean relative error 2.1%). In turn, SS concentrations were derived from K_d490 and backscattering at 550 nm. SS below 26 mg l^{-1} was estimated with an RMSE of ±3.3 mg l^{-1} while SS with values higher than 56 mg l^{-1} were poorly estimated with an RMSE of ±115 mg l^{-1}. Limitations of the model are due to the small number of *in situ* measurements, intrinsic uncertainties of satellite products, pixel size and within-pixel heterogeneity. The methodology was implemented in a new computer code which automatically calculates K_d at 490 nm, IOP (a and b_b) and SS from ocean color radiometric data from either SeaWiFS, MODIS or their merged products. Time series analysis of SS has revealed fluctuation patterns in the Rosario Island that can be related to specific peak in turbidity in the Magdalena/Sinu rivers. The developed method thus promises to be useful for monitoring marine ecosystems, ultimately contributing to adaptation strategies to climate and human-induced environmental change.

Acknowledgements

I would like to express my deepest gratitude to all institutions and persons who have given me their invaluable contribution during my research:

The Netherland Fellowship Programme that supported me financially to pursue my MSc studies.

The Marine and Costal Research Institute of Colombia for support my MSc application and for all logistic assistance during field work. I would like to thank all my friends and colleagues there: Francisco Arias Isaza, Paula Cristina Sierra, David Alonso, Daniel Rozo and Carolina Segura. Special thanks to Carolina Garcia who patiently assisted me in the field work and who shared with me the nice experience of seawater measurements.

I am most grateful to my first supervisor Dr. Suhyb Salama for his tireless critical guidance, encouragement, patience and thrust in my job. I have learnt a lot from you. Thank you very much.

My grateful thanks are extended to my second supervisor Dr. Chris M. Mannaerts and the water quality group, Syarif Budhiman and Wiwin Ambarwulan.

Special acknowledgement must go to Dr. Yves Thomas from CNRS -France, for their valuable guidance, for their assistance always with my questions and many other issues.

I thank all the staff at ITC, especially Prof.Dr. Z. Bob Su, Dr. David Rossiter, Drs. Boudewijn de Smeth and Dr. Mike McCall.

My deepest thanks to my husband, Fer. This study is the result of his support, encouragement, help and love. Gracias amor mio por seguirme y estar a mi lado!

Many thanks go to all our friends in ITC: all Colombian community, Latin friends and foreign friends. Especially to Marce, Ricardo, Ruben, Lucy, Diana, Guido, Marco…

Finally our family: Fanny, Max, Lili, John, Leo, Ana Tulia, Maria Victoria, Fernando and Alex, who encourage us with love through the distance.

Thanks God!

Table of contents

List of figures

List of tables

List of abbreviations

a	Absorption coefficient
b_b	Backscattering coefficient
CDOM	Colored dissolve organic matter
Chl-a	Chlorophyll- a
CNRS	National Centre for Scientific Research (France)
$Ed(0^-)$	Downward irradiance just below the surface
$Eu(0^-)$	Upward irradiance just below surface
$Ed(0^+)$	Downward irradiance just above surface
$Eu(0^+)$	Upward irradiance just above surface
INVEMAR	Marine and Costal Research Institute
IOP	Inherent Optical Properties
K_d	Diffuse attenuation coefficient
K_d490	Diffuse attenuation coefficient at 490 nm
L_{WN}	Normalized water leaving reflectance
MODIS	Moderate Resolution Imaging Spectroradiometer
SS	Suspended sediments
SeaWiFS	Sea-viewing Wide Field-of-view Sensor
SPM	Suspended particular matter
$R(0^-)$	Irradiance reflectance just below the surface
R_{RS}	Remote sensing reflectance
REDCAM	Network of Marine Environmental Quality

1. Introduction

Suspended sediments (SS) are an important factor in water quality monitoring. Their variations in coastal waters might imply problems such as, erosion of beaches, dynamic of coastline, alteration of harbor basins and degradation of marine ecosystem. Presence of SS causes reduction of available light to aquatic vegetation and provides substrate for transporting of organic and inorganic substance, (including pollutants) and becomes the main substrata for biochemical processes (Doerffer et al., 1989). This suspended matter can be from land-based runoff, coast erosion, atmosphere inputs and from the bottom stirred up by waves and tidal currents.

In the Colombian Caribbean Sea, the main influence of SS is due of discharge of Magdalena and Sinú rivers, affecting extensively its water quality (Restrepo and López, 2008; Restrepo et al., 2006). An important characteristic of the region is the presence of a coral reef protected area, Rosario and San Bernardo Islands, which is recognized as one of the most developed coral reef area in Colombia (Diaz et al., 2000). Increasing sediment load due to rivers discharge is an important cause of coral reef degradation and according to Restrepo et al (2006) both the entrained mud and the reduced salinity are considered to have caused acute damage to the coral reefs. Studies made by Andrade et al. (2005) and Bernal et al. (2006) analyze sedimentation process using sediment traps installed at Salmedina Bank (sector of Rosario Islands). They found more significant sedimentation patterns at south of the coral reefs, near to the mouth of one artificial arm of Magdalena river (Dique channel) and conclude that both temperature and sedimentation are stress factors for coral development at the area.

Ocean colour sensors offer a suitable tool for monitoring water quality. The main advantage of these techniques is the near-real time synoptic view of seawater biophysical properties for large regions allowing an estimation of general tropic state of the water. The three active optical factors that affect water quality are chlorophyll, suspended sediments and dissolved organic matter. Many studies have been carried out for estimation of concentration and distribution of these factors. In particular, for mapping distribution of SS a number of satellite instruments have been used, these include Coastal Zone Colour Scanner (CZCS) (e.g. Clark et al., 1980; Tassan and Sturm, 1986), Advanced Very High Resolution Radiometer (AVHRR) (e.g. Froidefond et al., 1993), Sea-viewing Wide Field-of-view Sensor (SeaWiFS) (e. g. Binding et al., 2003; Warrick et al., 2004), Moderate Resolution Imaging Spectroradiometer (MODIS) (Miller and McKee, 2004) and more recently Medium Resolution Imaging Spectrometer (MERIS) (e.g. Kratzer et al., 2008). According to Gordon and Wang (1994), determination of water turbidity based on radiative transfer equations provides the best spatial coverage possible and is the easiest way to observe water quality patterns in the marine environment.

From remote sensing viewpoint seawater might be classified in Case 1, in which concentration of phytoplankton is high and Case 2, where inorganic particles or dissolve organic matter from land drainage dominate (Gordon and Morel, 1983; Mobley, 1994). In near shore and coastal region with coral reef presence, water quality has the largest gradients from clear oceanic water (case 1) to turbid near shore waters (case 2) (Udy et al., 2005). Many studies have been made to provide a better understanding of coastal water quality and coral reef ecosystem dynamic. Mumby et al. (2004) make a broad review of environmental reefs properties that can be retrieved using ocean optics techniques. They claim that at meso-scales, changes in the water quality beyond reefs are detected daily using observations from ocean colour sensors. However, they affirm that further research is needed into the

use of ocean colour instruments to detect changes in the water column integrating Case 2 waters and shallow coastal regions where reflectance from seabed complicates the calculations of the water optical factors.

Models of light attenuation as the diffuse attenuation coefficient is of particular interest because it quantifies the presence of light and helps to characterize the water column. The use of diffuse attenuation functions (K_d) is promising (Smith and Baker, 1978) because it does not require absolute radiometric measurements since they are defined as ratios; K_d are strongly correlated with phytoplankton chlorophyll concentration, thus they provide a connection between biology and optics; about 90% of the diffusely reflected light from water body comes from a surface layer of water of depth $1/K_d$; thus K_d has implications for remote sensing.

Radiative transfer theory provides several useful relations between the K_d and other quantities of interest, such as the absorption and beam attenuation coefficients and other AOP's. In that sense, there have been a numerous studies carried out combining K_d assessment and remote sensing techniques (Kratzer et al., 2008; Lund-Hansen, 2004; Mélin et al., 2005; Mishra et al., 2005; Mueller, 2000). In particular, Udy et al. (2005) combine MODIS remote sensing image and sampling techniques to characterise the spatial variability of suspended sediments, light attenuation and chlorophyll a concentrations in the Great Barrier Reef of Australia. They found that K_d values obtained from the MODIS were in similar range as those determined by RAMSES measurement and similar to light attenuation observed for other near- shore systems with a similar gradient in water quality. Also, Segal et al. (2008) make a quantitative description of the processes that influence sediment to the Brazilian reefs using combination of SeaWiFS K_d 490 product, Landsat TM images, and in situ data.

With respect to scattering and absorption of light in turbid waters, some studies have attempted to understand their variability. Babin et al. (2003b) documented variations in the components of the absorption coefficient in different coastal region and diversity of spectral signature of suspended particle matters (SPM). They found exponential variations of dissolve organic matter and not algal particles. As well, Babin et al. (2003a) studied the variation in the spectral scattering coefficient of marine particles. They conclude that backscattering at 555 nm explains variations in suspended particles despite these are dominantly organic, which may result from higher absorption relative to scattering. Other studies have been carried out to asses these inherent optical properties (IOP) from satellite data (Loisel et al., 2002; Mélin et al., 2005; Stramski, 1999).

As far as is known, reliable ocean optics algorithms to retrieve suspended sediments are currently limited to sensors, season and site-specific. Colombia suffers from scarcity of reliable in-situ data on SS and water optical properties. There too few remote sensing method that can be used to estimate SS and study their effects on aquatic ecosystem. Optical colour applications have been done mostly for Case 1 waters using CZCS, NOAA and SeaWiFS (e.g. Andrade, 1995; Andrade and Barton, 2005). As well, quantification of suspended sediments distribution has been carried out using numerical modelling and mostly considering only the Magdalena river discharge (Cañon and Santamaria del Angel, 2003; Restrepo and Kjerfve, 2000; Restrepo and López, 2008).

Due to these facts, this study affords a new local optical model that relates the diffuse attenuation coefficient to concentration of SS and observed remote sensing reflectance for the Caribbean Sea offshore in Colombia. This approach is proposed because K_d establishes the link to marine biology, and thus the effect of SS on marine environment can be directly assessed. Multi sensors data provides a more complete temporal coverage avoiding data gabs due to cloud coverage. And the time series of

ocean color data help to understand the temporal variations of SS, some persistent patterns and the response of coral reef protected areas to high discharge of SS from Sinú and Magdalena rivers.

This model provides maps that facilitate monitoring of the temporal and spatial variations of the suspended sediment and contributes to the knowledge on multi spatial and spectral data assimilation techniques in tropical waters, specifically for suspended sediments applications.

This research is part of a larger study of Marine and Coastal Research Institute of Colombia (INVEMAR) and the National Centre for Scientific Research of France (CNRS). It aims to fulfill four main objectives: a) in situ measurements of the vertical flux using sediments trapping methods; b) simulate the muddy marine snow with numeric modelling; c) describe the hydrodynamic forces controlling the system, temperature, SS and sea coral bottom characterization using remote sensing and d) estimate vulnerability of coral reef to degradation. This study contributes in third and forth objectives.

1.1. Research objectives

The aim of the research is to retrieve suspended sediments concentration using optical modelling based on diffuse attenuation coefficient (K_d) and multi spectral, spatial and temporal data in coastal waters of the Caribbean sea, Colombia.

1.1.1. Specific objectives

- Developing a ocean colour ratio model to estimate the diffuse attenuation coefficient (K_d) for the Caribbean offshore affected by the discharge of Magdalena and Sinú rivers, Colombia.
- Measuring the threshold of available light in the study area using the diffuse coefficient at 490nm (K_d490) and merging multi spatial and spectral data.
- Estimating IOP and suspended sediments concentrations based on K_d490 local model.
- Assessing the spatial and temporal variability of the suspended sediment in the study area over the period of last 10 years (1998 – 2008).

1.1.2. Research questions

- Can empirical ocean colour ratio model estimate the diffuse attenuation coefficient for the study area?
- What are the values of the diffuse attenuation coefficient (K_d) for the Caribbean offshore affected by the discharge of Magdalena and Sinú rivers, Colombia?
- Can we relate the K_d490 directly to the IOP of suspended sediment in the study area?
- How the multi spatial and spectral data assimilation techniques can enhance retrieved information SPM on the temporal and spatial distribution for a better management of marine ecosystems?
- How is the spatial and temporal variability of suspended sediments in the study area over the period 1998-2008?

1.1.3. Hypothesis

Is feasible to develop an ocean colour local model to estimate the diffuse attenuation coefficient for the Caribbean offshore affected by the discharge of Magdalena and Sinú rives in Colombia.

Using the diffuse attenuation coefficient at 490 nm is likely to measure the threshold of available light in the study area.

Relation between K_d490 and absorption and backscattering coefficients allows retrieving suspended sediments concentration in the study area.

Multi spatial and spectral data assimilation techniques are suitable to measure the variability of the suspended sediments and they can be used as a tool for better management of marine ecosystems.

Variability of suspended sediments due to discharge of Magdalena and Sinú rivers is possible to be assessed for the period 1998 – 2008.

1.2. Thesis structure

The document is structured by chapters (Figure 1). First chapter describes the introduction including literature review and research objectives. Second chapter explains the method and theoretical background of this approach. Third chapter shows description of study area and the dataset employed during the research. Fourth chapter shows main findings and contributions of the research. In the fifth chapter the project is discussed and finally in chapter six conclusions and recommendations are expressed.

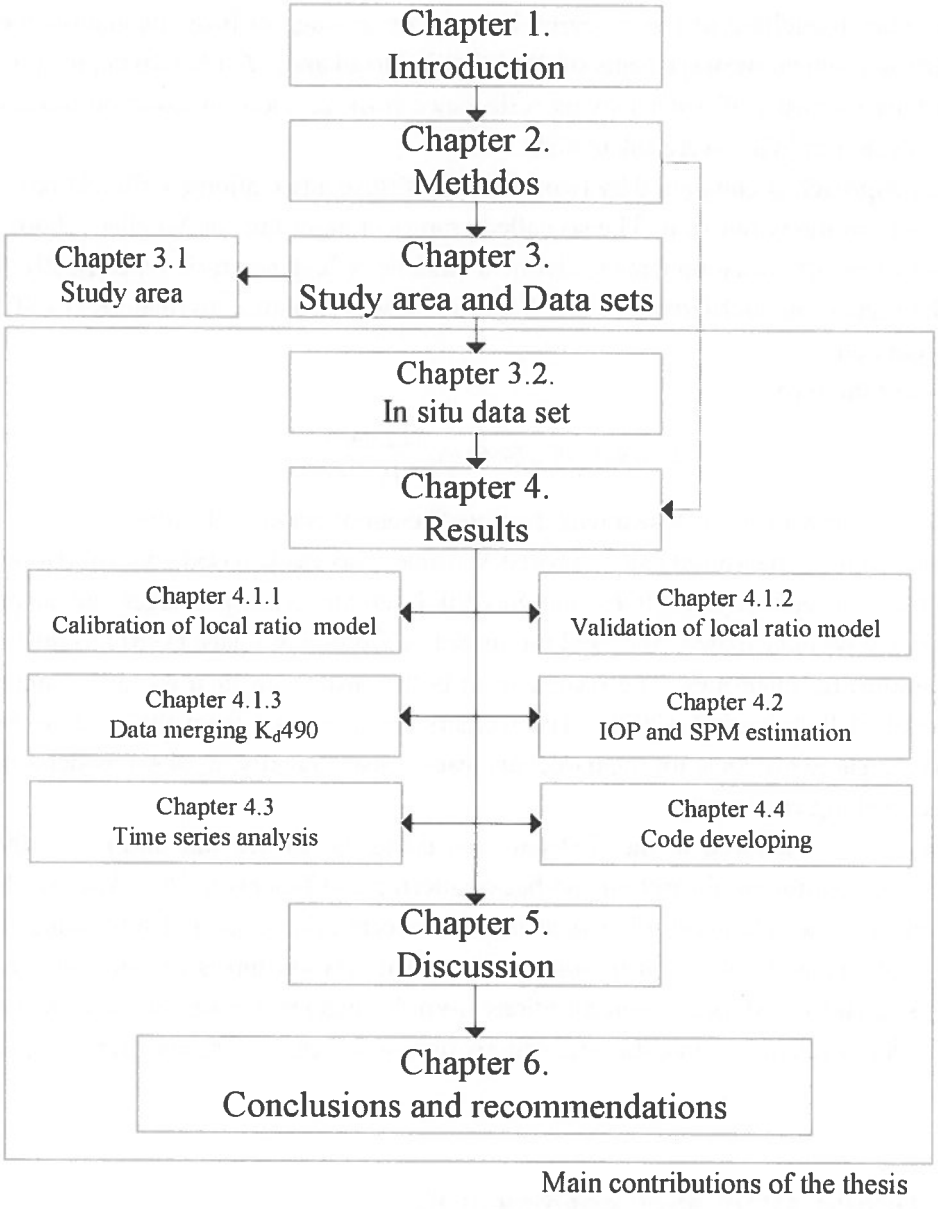

Figure 1 Structure and main contributions of the thesis

2. Methods

2.1. Proposed approach

The ocean optics modelling of this research is based on average diffuse attenuation coefficient (K_d), using underwater optical measurements of downwelling irradiance (E_d) in two depths (50 and 100 cm) and *in situ* measurements of water leaving reflectance (L_W). In addition, concentrations of suspended sediments and chlorophyll-a were calculated.

The research approach is compound by two parts, the diffuse attenuation coefficient retrieval, and IOP and SPM concentrations retrieval. The so called empirical algorithm of Mueller (2000), is calibrated with new set of *in situ* measurements to define a suitable reflectance ratio (specifically for SPM) and to derive the regression coefficients (α, β). Appropriate wavelength λ, to relate K_d to SPM, is defined during the research.

The model is of the form

$$K_d(490) = K_{dW}(490) + \alpha\left(\frac{L_{WN}(490)}{L_{WN}(\lambda)}\right)^{\beta} \quad (1)$$

Where K_{dW} is the downward diffuse attenuation coefficient of water molecules.

Error analysis between measured and estimated K_d values was made based on a validation set of *in situ* measurements. Subsequently, MODIS and SeaWiFS remote sensing images are acquired and the monthly average was calculated. We used the model of Gordon & Clark (1981) to relate measured to observed radiometric quantities. The results from both sensors are then merged using the weighted average model of Pottier et al. (2006). The weights are estimated from the relative errors between derived and measured products for the model and each sensor. Finally, K_d(490) model is applied to the set of images making error analysis.

Based on K_d values retrieved in the first part and using the Loisel and Stramski (2000) model, is performed the derivation of absorption and backscattering coefficients (a, b_b). Afterwards, scatter plot is used to analyse the relationship between *in situ* concentration data and IOP values (a, b_b). Error analysis is made using a validation in *situ* data set. That relationship is the base of the algorithm to retrieve the suspended sediments concentrations from the images. Finally, in order to understand the variability of SS in relation with coral reef waters, time series analysis is performed by wavelet model (Torrence and Compo, 1998).

2.2. Diffuse attenuation coefficient K_d

Under typical conditions, the various radiances and irradiances all decrease approximately (when elastic scattering is neglected) exponentially with depth, at least when far enough below the surface (and far enough above the bottom, in sallow water) to be free of boundary effects (Mobley, 1994). The depth dependence of downward irradiance (E_d) is governed by the Beer-Lambert Law, using the diffuse attenuation coefficient $K_d(z;\lambda)$ as:

$$E_d(z;\lambda) \equiv E_d(0;\lambda)\exp\left[-\int_0^z K_d(z';\lambda)dz'\right] \quad (2)$$

Solving $K_d(z;\lambda)$ gives

$$K_d(z;\lambda) = -\frac{d \ln E_d(z,\lambda)}{dz} \quad (3)$$

And defining $\overline{K}(\Delta z, \lambda)$ as the average diffuse attenuation coefficient for a water layer with Δz thickness, it can write as:

$$\overline{K}(\Delta z, \lambda) = -\frac{1}{\Delta z} \ln \frac{E_d(z_2,\lambda)}{E_d(z_1,\lambda)} : |z_2| > |z_1| \quad (4)$$

2.3. Water leaving radiance $L_W(\lambda)$ and normalized water leaving radiance $L_{WN}(\lambda)$

Most of the variables involved in the remote sensing of the ocean colour are based on, or derived from, the basic radiometric quantity often called water-leaving radiance $L_W(\lambda)$, defined as the radiance which emerges from the ocean, determined just above the water-air interface at a level 0^+ (Morel and Mueller, 2003). However, as $L_W(\lambda)$ is dependent on the surface boundary conditions and IOP of the water body, Gordon and Clark (1981) attempting to account its bidirectionality condition, defined the normalized water-leaving radiance $L_{WN}(\lambda)$, that is the radiance which would be observed if the sun was at zenith and at mean earth-sun distance and there was no atmosphere.

$$L_{WN}(\lambda) = \frac{L_W(\lambda)}{E_d(0^+)} \overline{F_0} \quad (5)$$

Where $\overline{F_0}$ is the solar irradiance at the top of the atmosphere at the mean sun-earth distance (d_0).

2.4. Empirical algorithm for K_d at 490 and radiance ratio

The diffuse attenuation coefficient $K_d(490)$ has been developed by Mueller (2000) based on the ratio of water leaving radiances at 490 and 550 nm. Some variations in coefficients have been proposed by Berthon et al. (2002) that seems an alternative more suitable for coastal waters (0.15645 by 0.205 and -1.5401 by -1.754).

$$K_d(490) = 0.016 + 0.15645 \left(\frac{L_{WN}(490)}{L_{WN}(550)} \right)^{-1.5401} \quad (6)$$

The offset of 0.016 m^{-1} is the constant adopted for pure seawater.

2.5. Data merging

The merging of ocean color data sets allows data from multiple sensors to be used to derive unique sets of products and, in essence, is the method for creating unified ocean color time series (Maritorena and Siegel, 2005a). It can be performed either on radiometric quantities or biophysical derived products. Pottier et al (2006) proposed a merging method for SeaWiFS and MODIS/Aqua using error-weighted averaging. The method improved the spatial coverage by taking into account only the existing satellite values and it consumed low CPU time.

The original proposal of Pottier et al. (2006) was made for Chlorophyll-a product considering probabilistic function to measure the errors, present study modifies their method using K_d product and relative error as following:

$$K_d merged = \left(1 - \frac{\%ES}{\%EM + \%ES + \%EModel}\right) K_d S + \left(1 - \frac{\%EM}{\%EM + \%ES + \%EModel}\right) K_d M \quad (7)$$

Where K_d merged is the combined K_d product, %E is the mean of relative error (%EX = ((K_d Measured- K_d Estimated)/ K_d Measured)*100%), S for SeaWiFS data, M for MODIS data and Model for K_d 490 ratio model. The errors were estimated from derived and measured K_d values.
As MODIS and SeaWiFS L_{WN} products have different spatial resolution, downscaling process was performed by averaging. Relation between pixel sizes is: 2x2 pixel MODIS = 1 pixel SeaWiFS.

2.6. Relation between K_d, IOP and R(0⁻)

Loisel and Stramski (2000) developed a model based on radiative transfer simulations to estimate the absorption a, the scattering b and the backscattering b_b coefficients in the upper ocean from irradiance reflectance just beneath the sea surface $R(0^-)$ and the average attenuation coefficient for downwelling irradiance K_d between the surface and the first attenuation depth. An important feature of this model is both $R(0^-)$ and K_d can be estimated from satellite measurements of ocean color. Simulations performed for a homogeneous water column and solar zenith angle lower than 60° ($0° < \theta < 60°$) the errors in the model are on average 2.4% for a (maximum 6.5%), 8.5% for b (maximum of 23%) and 6% for b_b (maximum 20%).

Important aspect of present model is it takes into account the upper oceanic layer between the surface and the first attenuation depth and generates 90% of the water leaving upward photons, which can be detected by satellite sensors. Moreover, absorption and backscattering are considered as total.

In addition of $R(0^-)$and K_d measurements, the model requires knowledge of the solar zenith angle and requires the hypothetical reflectance if there were no elastic scattering. Moreover, retrieval of a and b_b is weakly depended on possible variations of the particle scattering phase function in the ocean. Estimation of the total scattering coefficient can be significant. The authors suggest caution to use the model for estimating b. In IOCCG (2006) some modifications of this model are exposed and the authors express that such modifications are for better retrieval of a and b_b in the context of ocean color remote sensing applications. The modify model is based on the following set of equations between a, b_b, K_d and $R(0^-)$:

$$a = \frac{\mu_w \overline{K_d}}{\left[1 + (2.54 - 6.5\mu_w + 19.89\mu_w^2)\frac{R(0^-)}{1 - R(0^-)}\right]^{0.5}} \quad (8)$$

$$b_b = \overline{K_d} 10^{\alpha} [R(0-)]^{\delta} \quad (9)$$

$$\alpha = (-0.83 + 5.34\eta - 12.26\eta^2) + \mu_w (1.013 - 4.124\eta + 8.088\eta^2) \quad (10)$$

$$\delta = 0.871 + 0.40\eta - 1.83\eta \quad (11)$$

where μ_w is the cosine of the refracted solar beam just beneath the surface and ,η is the ratio of molecular scattering to the total scattering (b_w/b).
For a and b_b monthly calculations were assumed θ = 28 as monthly average according to MODIS AQUA equator crossing time (1:30 pm) and η = 0.2 according to Mobley (1994).

2.7. Irradiance reflectance *R(0-)*

With the aim to estimate irradiance reflectance just below the sea surface $R(0^-)$ from the irradiances measurements (E_d100^-, E_d50^-, E_d0^+) was assumed an homogenous water column and constant diffuse attenuation coefficient. Thus, relation among K_d and E_d is as follow:

$$E_d 0^- = \frac{E_d(50^-)}{e^{-Kd*0.5}} \quad (12)$$

Then transferring the function from upward irradiance just below the sea surface $E_u(0^-)$ to above water $E_u(0^+)$:

$$E_u 0^- = \frac{1}{0.543} Eu0^+ \quad (13)$$

where E_u0^+ is defined direct from relation $E_u0^+ = L_{WN} * E_d0^+$.

On the other hand, to calculate the irradiance reflectance $R(0\text{-})$ from monthly L_{NW} from images, the water leaving reflectance L_{NW} is converted to remote sensing reflectance R_{RS}, using the following relation:

$$R_{RS}(\lambda) = L_{WN}(\lambda) / F_0(\lambda) \quad (14)$$

where F_0 is mean solar irradiance. For standard processing NASA (2009) reports nominal band values by sensor and wavelength (Table 1):

Table 1 Mean Solar Irradiance SeaWiFS and MODIS

SeaWiFS		MODIS	
Wavelength(nm)	**mW/cm^2/um**	**Wavelength(nm)**	**mW/cm^2/um**
412	171.18	412	171.18
443	188.76	443	188.76
490	193.38	488	194.18
510	192.56	531	185.94
555	183.76	551	187.00
670	151.22	667	152.44
765	123.91	748	127.60
865	95.965	869	94.874

Adapted from NASA (2009)

Therefore, R_{RS} is set in terms of irradiance reflectance $R(0^-)$ using the relationship proposed by Morel and Gentili (1993) and Lee et al. (1999):

$$R_{RS}(\lambda) = \frac{1}{Q} \frac{X * R(0^-)}{1 - Y * R(0^-)} \quad (15)$$

Where $Q = 5$ (Morel and Gentili, 1993) and $X = 0.54$ - $Y = 1.5$ (Lee et al., 1999).

2.8. Time series analysis

In order to perform time series analysis was used a Wavelet Analysis tool developed by Torrence and Compo (1998)[1]. This method is for analyzing localized variations within a time series by decomposing them into time frequency space. It includes functions such as:

- Windowed Fourier Transform (WFT): to extract local frequency information from a signal.
- Wavelet Transform: to analyze time series that contain nonstationary power at many different frequencies
- Wavelet power spectrum: to show variations in the frequency of occurrence and amplitude of specific events.

[1] Wavelet software available at URL: http://atoc.colorado.edu/research/wavelets/

- Cone of influence: to understand the region of the wavelet spectrum edge effects become important in terms of errors
- Scale-averaged wavelet power: to show average over all scales that gives a measure of the average variance versus time. This tool is specific to examine fluctuation in power over a range of scales and can be defined as the weighted sum of the wavelet power spectrum over scales. It can be called time series of the average variance in a certain band. It is used to examine modulation of one time series by another, or modulation of one frequency by another within the same time series.

More details about wavelet analysis model approach in Torrence and Compo (1998).

3. Study area and data sets

3.1. Study Area

The study area is located in the Caribbean Sea, northern part of Colombia (Figure 2). The coast line is approximately 370 Km from southwest Caribbean coast in close proximity to Sinú river mouth (76.3 W, 9 N) until the Magdalena river mouth (74.7 W, 11 N). Its seawater is warm and relatively not very deep, with complex environmental characteristics determining big amount of species and endemism. This semi enclosed sea has a stable thermocline almost through the entire year, perturbed only by winds and currents (INVEMAR, 2003).

One characteristic of the study area is the presence of the Rosario and San Bernardo Coral Reef National Park. The weather conditions (winds, currents, etc) have originate numerous environments and biotic associations that make this region one of the most developed coral reef area en Colombia.

Coral reef area is compound for three main subareas. Nuestra Señora del Rosario Islands, located at southwest part of Cartagena city, characterized by a rich coral reef development bordering the continent and around of Rosario Islands. There is evidence of some coral decline and even extinction due to Dique channel load (artificial arm of Magdalena River). Tortugas Bank, located between the two archipelagos, with an elongated shape (14 * 3.5 Km) growing up from the bottom at 100 m until 5 m of depth. Here there is a recent coral reef development. And San Bernardo Islands, the most developed coral reef area located in the southern part of the Park. It is dominated by a huge diversity of species in a superficial platform compound for 9 small islands (Diaz et al., 2000).

The Caribbean Sea is influenced by a considerable amount of fluvial contribution from Sierra Nevada de Santa Marta, Magdalena, Atrato and Sinú rivers, all of them influencing silt distribution, material exchange and dynamics of physical process (INVEMAR, 2003). Magdalena River is 1612 km long and drains a 257.438 km^2 basin. It is the largest fluvial system in Colombia and its basin occupies a huge portion of the Colombian Andes (Restrepo and Kjerfve, 2000). Sinú River is born on west mountain range and its longitude is 380 km draining 13700 km^2 (Ruiz-Ochoa et al., 2008).

The study area is characterized by moderate rainfall (mean 2050 mm yr -1). There are two dry seasons of low rainfall on December-March and June-September, and two wet seasons of high rainfall on March-May and October-November (Restrepo and Kjerfve, 2000).

The water discharge and sediment load of Magdalena and Sinú rivers are depicted in Figure 3. For Magdalena River it was used the data of hydrological station named Calamar, located 112 km upstream from the Caribbean[2]. According to data for period 1941 – 2000, there is a mean annual water discharge of 6361 m^3s^{-1} with a mean low discharge of 4068 m^3s^{-1} in March and a mean high discharge of 10287 m^3s^{-1} in November. These values differ to reported by Restrepo and Kjerfve (2000) and other studies, where a mean discharge is 7100 m^3s^{-1}. The reason of the difference possibly is related

[2] Information system of Institute of Hydrology, meteorology and environmental studies (IDEAM, Colombia), URL: http://ideam.org.co/

with the period of time (1975-1995). In terms of sediment load for Calamar station are two high values one in November of 690 x 10^3 t day^{-1} and other in June 443 10^3 t day^{-1}.

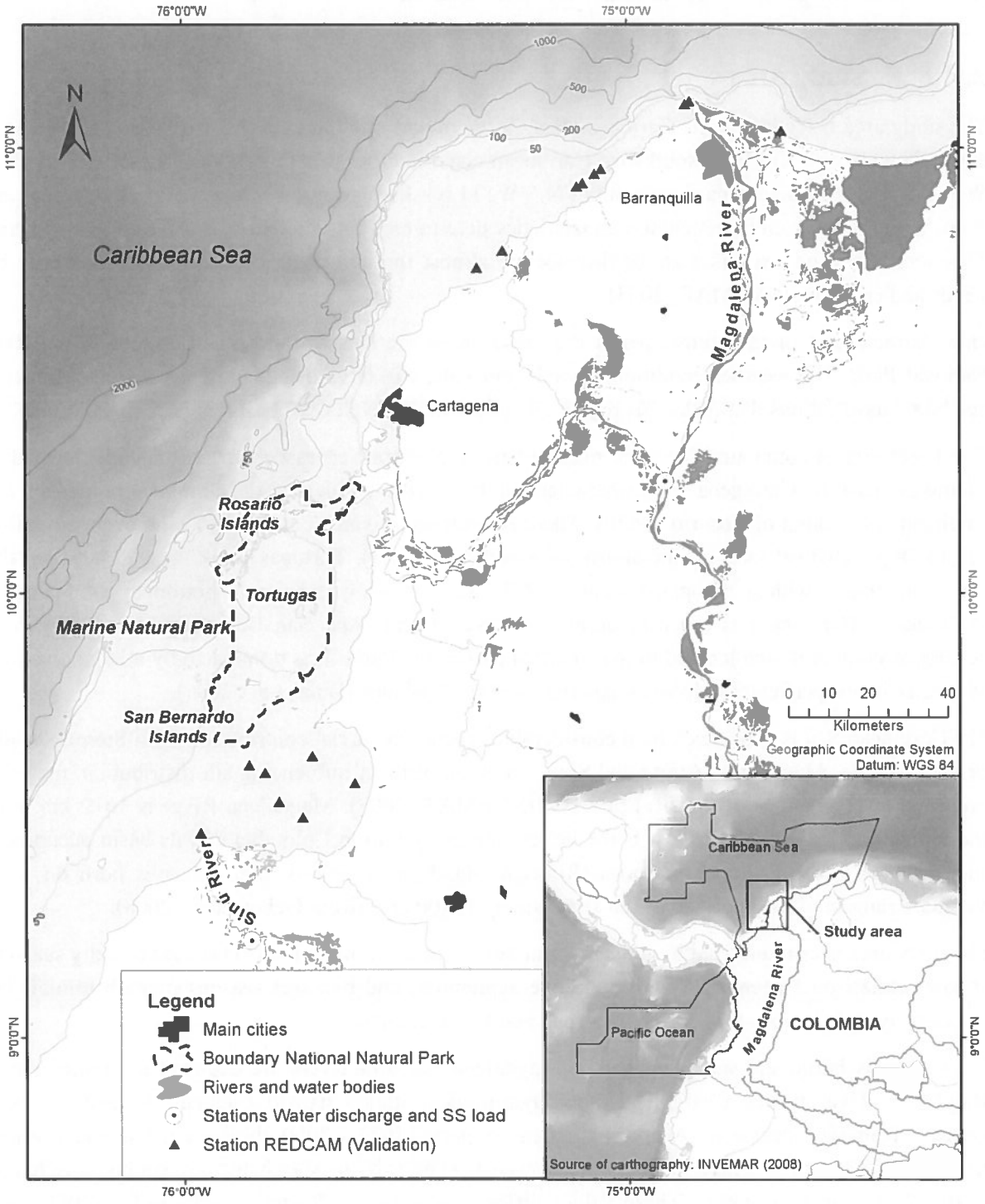

Figure 2 Study area (Source cartography INVEMAR (2008))

On the other hand, for Sinú River, water discharge and sediment load data are from Cotoca Abajo station, located 43 Km upstream from the Caribbean. According to the data, the annual water discharge of Sinú River is 233 m^3s^{-1}, the mean low discharge in March of 75 m^3s^{-1} and maximum discharge in October of 348 m^3s^{-1} (Figure 3), although the water discharge is showing high values

between July and November. Sediment load data indicates two peaks in July and November; this last is showing a high standard deviation due to high load in some atypical years (1992, 1998) that could be related with El Niño phenomena.

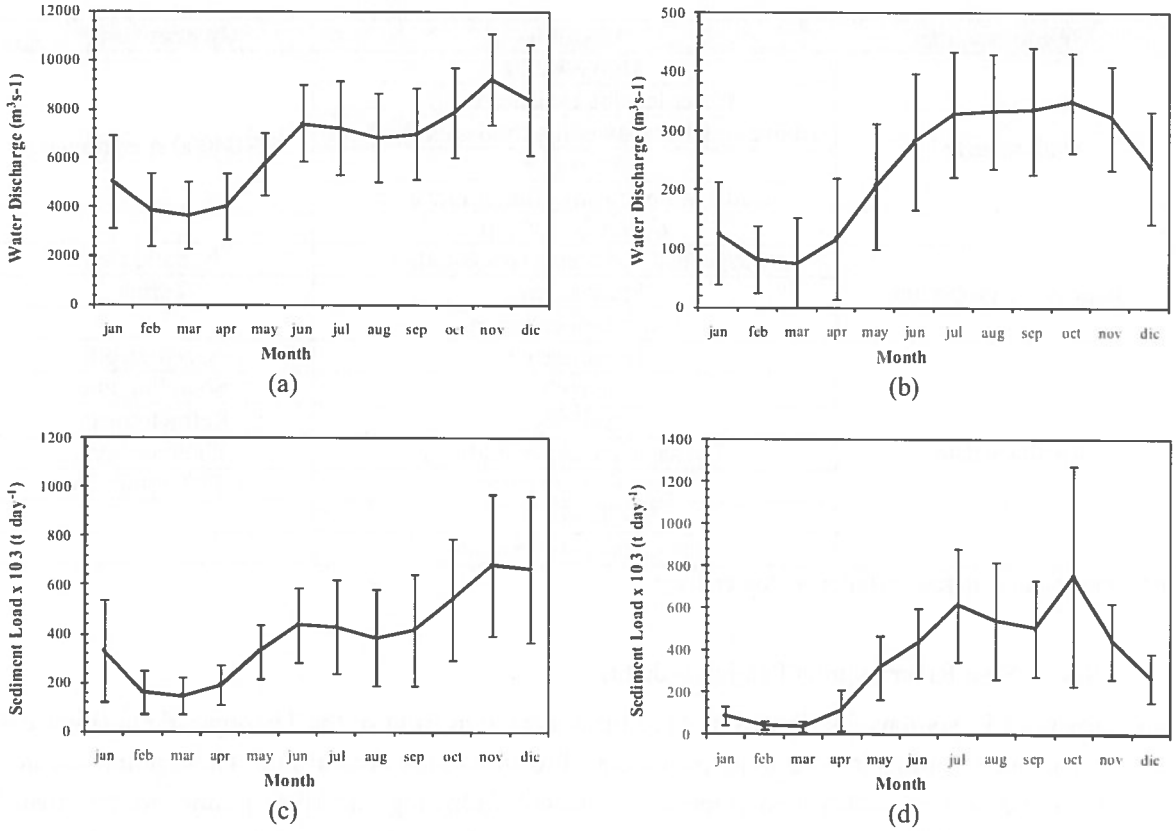

Figure 3 Monthly mean and standard deviation of water discharge (1941-2000) and sediment load (1984-2000) of Magdalena (a,b) and Sinú rivers (c,d)

3.2. Data sets

3.2.1. In situ measurements

The in situ data were acquired from 20 to 25 September, 2008. Radiometric variables measured were water leaving reflectance L_W (λ), downwelling irradiance $E_d(0^+)$ and downwelling irradiance $E_d(z,\lambda)$ in two depths (z_1 = 50 cm, z_2 = 100 cm). As well, water samples were taken for calculation of suspended sediments concentration in all stations and chlorophyll-a concentration only for Magdalena river stations (Table 2). Other ancillary data such as fluorescence, transparency, depth, salinity, sky and sea conditions, locations of the stations and cloud coverage were also measured in situ. At the end of each journey filtering process was performed using the filtration set.

Three sampling sites were selected according to the runoff of the Magdalena and Sinú rivers and the locations the coral reef area. In order to set sampling sites were followed next criteria:

- Locations and accessibility of Magdalena and Sinú mouths
- Bathymetry avoiding bottom reflectance
- Distance to the coastal line avoiding adjacency effect from the land
- Profiles from optically shallow to optically deep waters, making lines among 5 to 20 km with 1 kilometer of distance between sampling points. Direction and longitud of transects were estimated using a Landsat image of 2002 (Figure 4)

- Distance between points chosen as a trade off different spatial resolutions of the used EO data, varying between 1 and 9 km

Table 2 Measurements taken in the field

Measurements	Variable	Instruments*
Radiometric	**Above-water**	USB4000 spectrometer
	Water leaving radiance L_W (λ)	
	Above water downwelling irradiance $E_d(0^+,\lambda)$	
	In-water	
	Under water downwelling irradiance $E_d(0.5,\lambda)$, $E_d(1,\lambda)$	
Biophysical properties	Suspended sediments concentration	Filtration set
	Fluorescence	Turner
	Chl-a concentration	
Ancillary data	Transparency	Secchi depth
	Depth	Sounding line
	Salinity	Refractometer
	Sea state and sky conditions	Photo camera
	Location of station	GPS Garmin 76s
	% Cloud cover	
	Name, date, observations.	

*Instruments and materials detailed in Appendix A

- Site 1: Sinú River mouth (Tinajones delta)

It was measured 17 stations distributed in three lines located in front of the Tinajones delta (Figure 4). The first line had 11 points located in perpendicular direction to the coastal line. These points included clear and turbid waters. Other two lines were located following the river plume border, mainly between medium and high turbidity. First day of sampling the weather conditions were mainly rainy and the cloud coverage was 100% most of the time. On second day the cloud coverage varied between 20 to 70%.

- Site 2: Magdalena River mouth (Puerto Colombia and Bocas de Ceniza)

In Magdalena river site were measured 16 stations, 6 in front of Puerto Colombia city and 10 in the mouth of the river, region named Bocas de Ceniza (Figure 4). On first day of measurement, it was searching the Magdalena river plume in northeast direction, according to Landsat image of 2002. After 25 km of ride the plume did not become visible because it was in northwest direction. For this reason, first transect was in front of Puerto Colombia city where it was found mainly low turbid waters. For second day, the route started in the Magdalena River itself, going out to Bocas de Ceniza. The weather and sea conditions were ideal to make the first station approximately 500 meter to the coastal barrier. Around mid day there was a 2 hours storm which changed the water conditions and plume direction (southwest). In order to include data from high and low turbid waters, it was followed two parallels lines of 5 km to southwest direction, crossing the plum. For this station group was taken water samples to determine chlorophyll-a concentration.

- Site 3: Rosario Islands

In Site 3 it was measured 10 stations on a straight line with northeast direction. First station was located 1 kilometer from Tesoro Island. Most of the time cloud coverage was near to 0% and waves and currents were soft. All the data was taken avoiding sea bottom reflectance, the depth in the area is more than 70 meter.

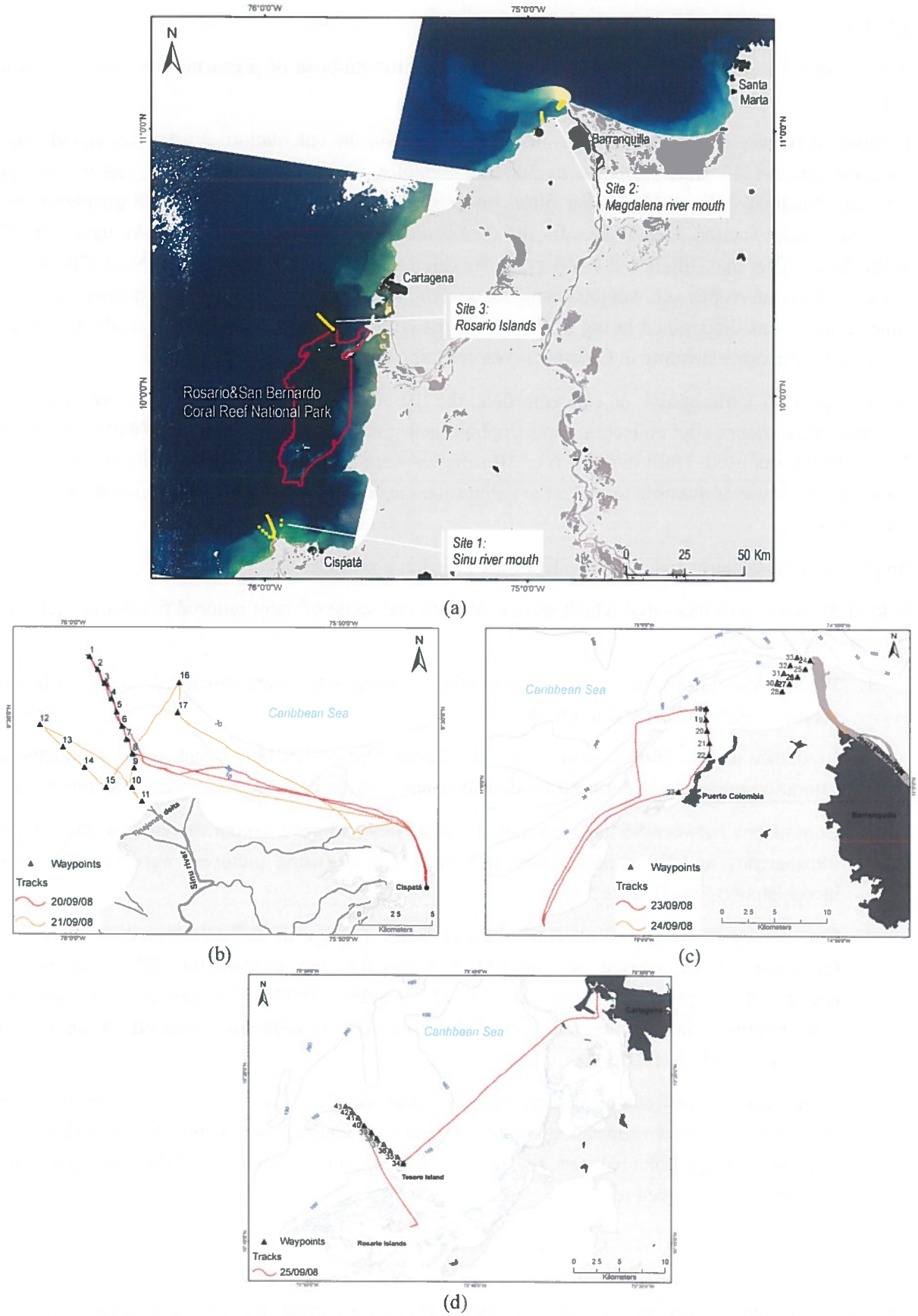

Figure 4 Field work maps. (a)Landsat Image 2002 (b) Sinú river mouth (c) Magdalena river mouth (d) Rosario Islands

3.2.1.1. Analysis of in situ data

After field work, some activities were completed with the purpose of preparing the data for further steps.

In terms of biophysical measurements, first was performed the calculation of total suspended solids concentration for 43 water samples of 500 ml. Samples were filtered through a pre-washed and weighed Whatman 1.6 µm Microfiber filters under suction. Filters were washed with distilled water, while still under suction, to remove salts and then placed in aluminium envelope (tasks made directly in the field). After that, filters and envelopes were dried for 24 hours at 105°C oven. Next, filters were removed from envelopes and weighed using an analytic balance (0.0001 g), the total suspended solids concentration was determined in mg l^{-1}. For the process it was followed standard protocol of Marine and Coastal Research Institute in Colombia (Garay et al., 2003)

With respect to Chlorophyll -a concentration, the 10 water samples of 2 liters were sent to a Laboratory two hours after collection. Spectrophotometric standard method (AWWA/APHA/WEF/ED 21 10200 H) was used. Unfortunately 6 of 10 samples were under detection threshold (0.10 mg m^{-3}) consequently it was unfeasible to make the calibration curve of fluorescence measurements and Chl-a concentration.

Biophysical, radiometric and ancillary data were saved in a personal data base in Excel.

In total 43 point were measured which were evaluated and some of them ignored following exclusion criteria (Appendix B):

1. Weather conditions: the measurements taken in rainy days were discarded, in particular for measurements of first and fourth day.
2. Irradiance measurements saturation: the Ocean Optics USB4000 had some problems of saturation mainly in high turbid irradiance samples, those measurements were not considered.
3. Consistency between SS concentration, transparency and water colour: based on scatter plot of transparency and SS concentration and water colour (using pictures) were rejected some inconsistent points (Figure 5).
4. Consistency between SS concentration and $K_d(\lambda)$: average of diffuse attenuation coefficient (equation 4), was carried out for 490, 555 and 670 nm, considering diffuse attenuation coefficient of pure sea water as 0.0212 (Mobley, 1994). Comparing $K_d(\lambda)$ and SS concentration some points were rejected taking into account the expected fitting with a logarithm function (Figure 6).
5. Water leaving reflectance saturation: the reference files for L_W were incorrectly saved presenting saturated reflectance curves. In order to figure it out, white (R_λ) and dark (D_λ) references in equation (16) were replaced by standard solar irradiance and the minimum of the ratio of S_λ / R_λ, respectively.

$$\%Lw_{(\lambda)} = \frac{S_\lambda - D_\lambda}{R_\lambda - D_\lambda} * 100\% \quad \textbf{(16)}$$

After above evaluation process, 11 stations remained with a correct and complete radiometric and biophysical data. This in situ dataset was divided in two groups, one for calibration (6 stations) and

one for validation (5 stations). Moreover, 9 stations with only irradiance measurements used for $K_d(\lambda)$ average calculation and SMP concentration validation.

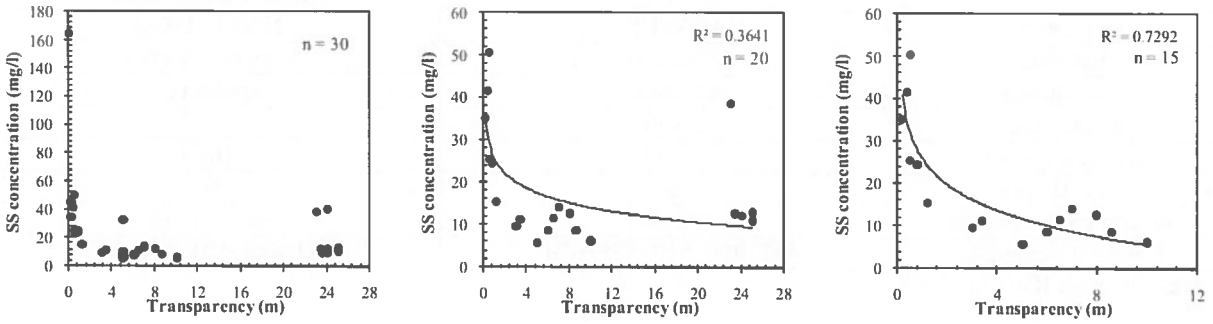

Figure 5 Comparison between transparency and SS concentration for n = 30, n = 20 and n = 5

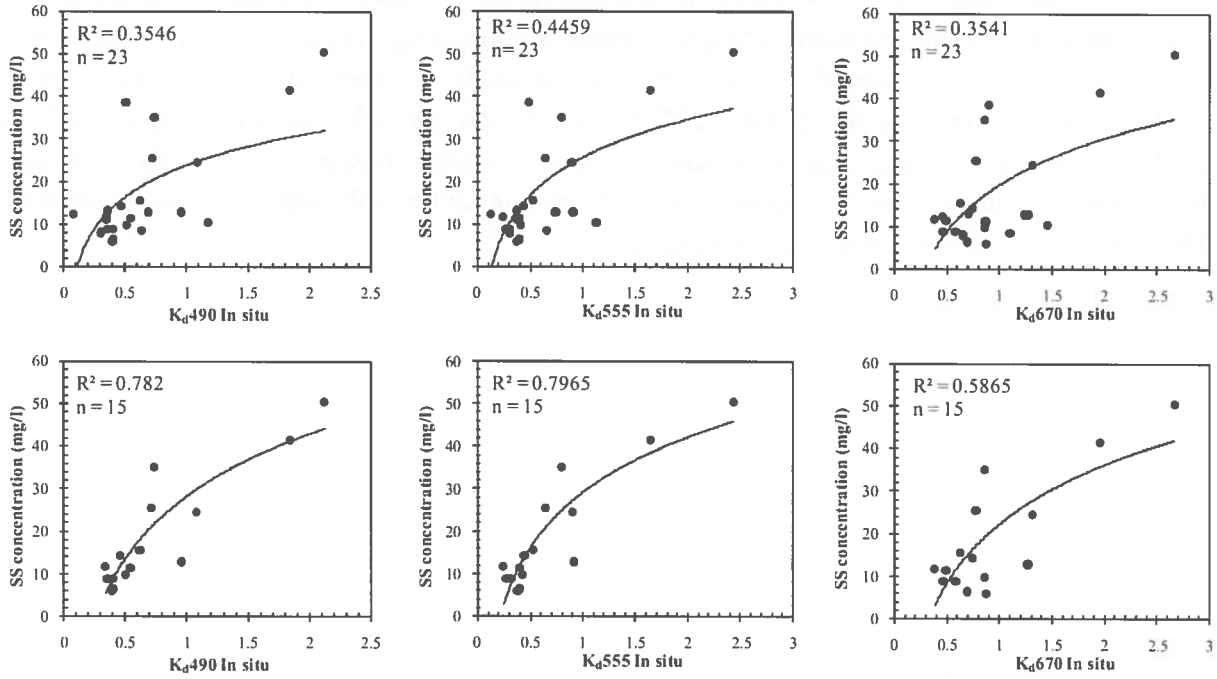

Figure 6 Comparison between diffuse attenuation coefficient and SS concentration at 490, 555 and 670 nm for n = 23 and n = 15

3.2.2. Satellite data

The satellite product used in this study was the Normalized Water Leaving Radiances (Level 2) obtained from SeaWiFS (Sea Viewing Wide Field of View Sensor) for 1998 – 2008 and MODIS (Moderate Resolution Imaging Spectroradiometer) for 2002-2008. Some technical specifications of these two sensors are illustrated in Table 3.

According to Gordon and Wang (1994), the normalized water leaving radiance is the product used in algorithms to produce geophysical values, such as chlorophyll and suspended sediment concentration. It is defined as the radiance that would be measured exiting the flat surface of the ocean with the Sun at zenith (directly overhead) and the atmosphere absent since about 10% of the total light detected by a satellite aimed at the ocean is water-leaving radiance, while the other 90% of the light is due to atmospheric effects. Once the radiance signal has been corrected for atmospheric light scattering, the signal is then corrected for the solar zenith angle.

Table 3 Specifications of satellite data

	SeaWiFS	MODIS
Name	Sea-viewing Wide Field-of-view Sensor	Moderate Resolution Imaging Spectroradiometer
Agency	NASA (USA)	NASA (USA)
Satellite	OrbView-2 (USA)	Aqua (EOS-PM1)
Launch date	01/08/97	04/05/02
Swath (km)	2806	2330
Resolution(m)	1100	1000
# Of Bands	8	36
Spectral coverage (nm)	402-885	405-14385
Center wavelength	443, 490, 510, 555, 670	443, 488, 531, 551, 667

Adapted from IOCCG (2008)

3.2.3. Marine and coastal water quality database

The water quality database, REDCAM has been implemented by Marine and Costal Research Institute in Colombia since 2000. The REDCAM is developed for monitoring marine and coastal water quality by measuring systematic variables in superficial coastal waters and continental waters (Garay et al., 2001). In the study area for period 2000-2007 there are 16 stations with around 150 measurements of SS. About 86 measurements are from marine waters. Sampling strategy is half-yearly, measuring between March and June for first semester, and between September and October for second semester. Data are available online in www.invemar.org.co.

4. Results

This chapter describes the main finding of present research. It starts with description of the results obtained by application of the developed model for K_d retrieval. The application includes calibration, validation and data merging. Then, results of IOP and SPM estimation and its implications are explained. Finally we carried out wavelet time series analysis.

4.1. K_d retrieval

4.1.1. Calibration of local ratio model

Calibration of K_d490 ratio model was performed with in situ measurements and regression analysis. Three ratios, L_{WN}490/550, L_{WN} 490/555 and L_{WN} 490/670 were tested to find the suitable reflectance ratio specifically for SPM, since original Mueller (2000) empirical model was proposed for range of K_d between 0.016 to 0.25 m^{-1} while present study handles a higher K_d range 0.07 to 2.1 m^{-1}(Figure 7).

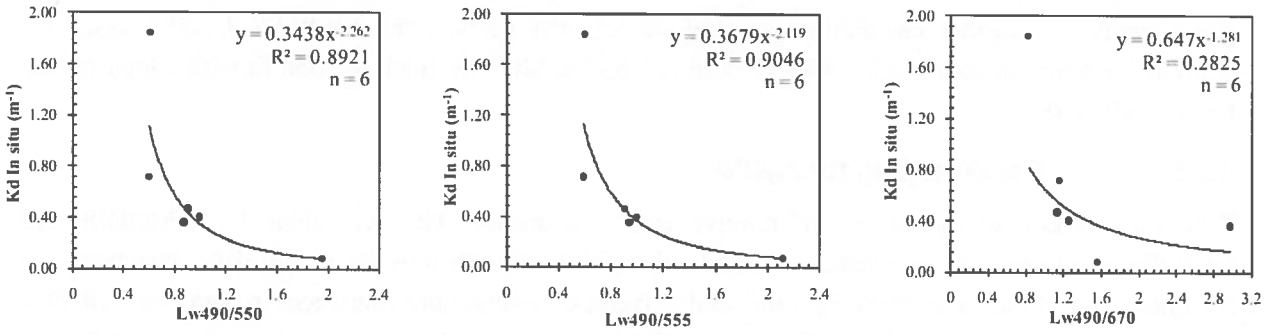

(a) (b) (c)

Figure 7 Ratio model calibration, (a) 550, (b) 555 and (c) 670 nm

The results have shown higher correlation coefficient (R^2) for 555 nm and lower for 670 nm, however difference between 550 and 555 is not significant (Table 4).

Table 4 Regression coefficients three $L_{WN}(\lambda)$ ratios derived from calibration

	α	β	R^2
Ratio L_{WN}490/550	0.3438	-2.262	0.89
Ratio L_{WN}490/555	0.3679	-2.119	0.90
Ratio L_{WN}490/670	0.647	-1.281	0.28

4.1.2. Validation of local ratio model

Validation was performed with 5 points calculating relative error, mean square error, root mean square error and correlation coefficient. As well, models of Mueller (2000) and Berthon et al. (2002) were tested using same validation data set and using whole data set (11 points). Results are described in Table 5. Although, correlation coefficients for the three models are significantly good, near to 1, the mean relative error is significantly improved for present study comparing with other two models, it varies from 59,8% using Mueller's model to 1.15%.

Table 5 Validation K_d Model

Validation data set			
	Present Study	**Mueller (2000)**	**Berthon et al. (2002)**
α	0.3679	0.1564	0.2050
β	-2.119	-1.5401	-1.7540
Mean relative error (%)	-1.150	-59.884	45.533
MSE	0.024	0.247	0.166
RMSE	0.154	0.497	0.408
R^2	0.982	0.982	0.996
Calibration + Validation data set			
Mean relative error (%)		-52.270	-36.624
MSE		0.576	0.446
RMSE		0.759	0.668
R^2		0.822	0.825

Therefore, K_d calculation was performed on MODIS and SeaWiFS monthly images following equation (1), values adopted for α and β were 0.3679 and -2.119. The results are monthly K_d490 images for each sensor.

SeaWiFS L_{WN} images presented a persistent error in monthly average. This was probably caused by missing data or troubles in Level 2 algorithm. It made impossible to employ those images in K_d calculations. To figure it out, it was derived the ratio L_{WN} 490/550 from K_d 490 SeaWiFS product. Additionally, for further calculations in IOP model, was derived the SeaWiFS $L_{WN}555$ based on relationship between the ratio $L_{WN}490/555$ and L_{WN} 555 in MODIS. Such relation fit with a logarithmic function ($R^2 = 0.78$).

4.1.3. Data merging for K_d490

With the purpose of calculation of relative errors associated with K_d values from MODIS and SeaWiFS, locations were extracted (row and column) of the matchups for in situ data. Matchups are considered as these coincident in time and coverage observations between in situ and satellite measurements (Pottier et al., 2006). For K_d (satellite data) the monthly average of September 2008 was considered and for *in situ* data the average of coincident points per pixel. Then, associated relative and absolute errors were measured (Appendix C). Based on these errors and using equation (7), K_d merged product was determined. Previous to K_d merged calculation, MODIS images were dimensioned to SeaWiFS size (4 km).

Error analysis for K_d merged product was performed as well using matchup in situ points, results are showed in Table 6. The analysis indicated high mean relative error for K_d MODIS, more than 50% of underestimation, and considerably low for K_d SeaWiFS (3.3%). After merging process the relative error is significantly improved with positive value of 2.5%.

Table 6 Relative errors for K_d MODIS, SeaWiFS and merge

Errors	MODIS	SeaWiFS	Merge
MSE	0.094	0.077	0.085
RSME	0.306	0.277	0.291
Mean relative error (5%)	-50.555	-3.311	2.541

In spite of the losses of information due to downscaling, evident information was gained in cloud covered areas. Figure 8 shows two examples of K_d monthly products from MODIS (upper part), SeaWiFS (middle) and merged product (lower part) where is possible to observe this fact.

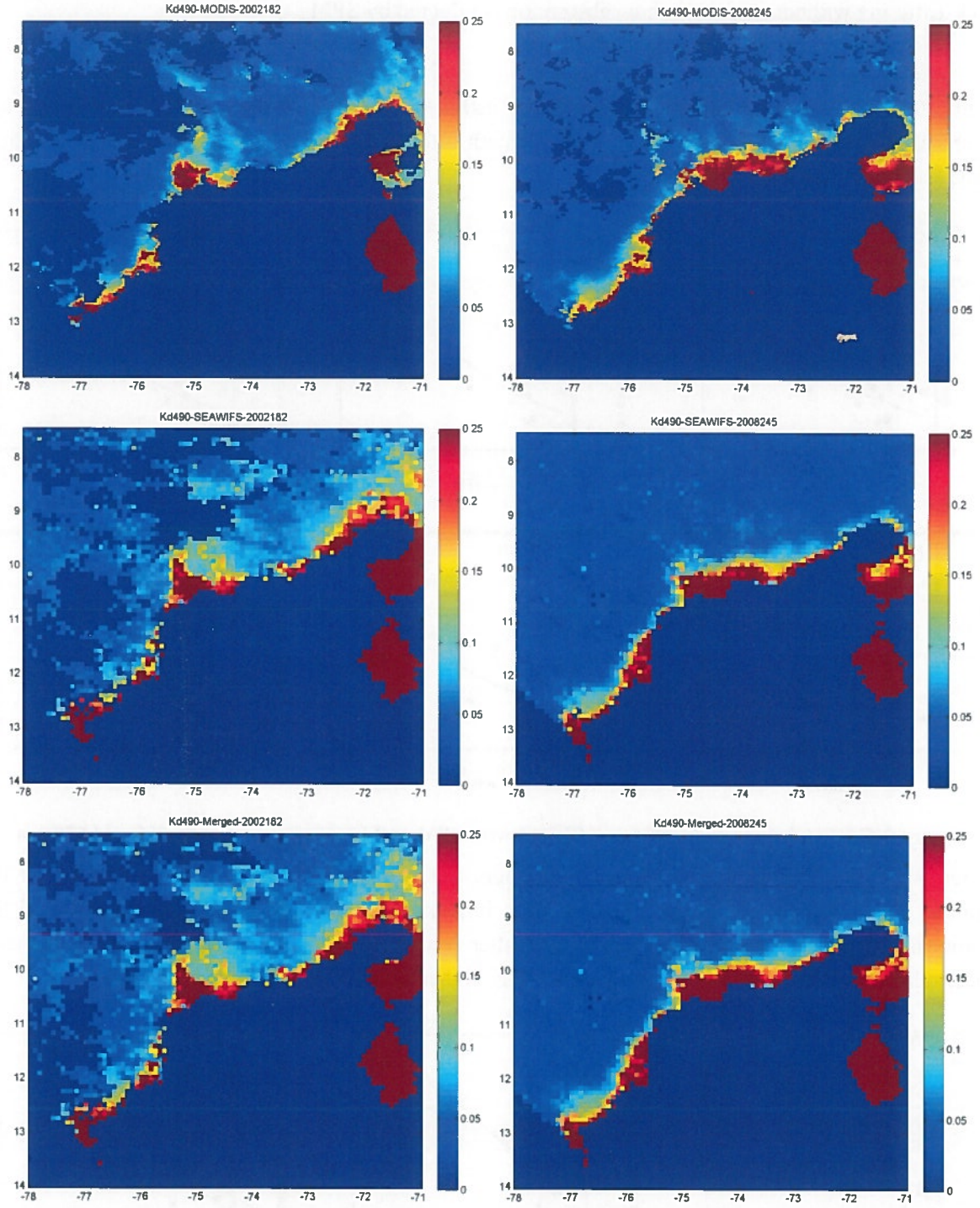

Figure 8 Examples of MODIS, SeaWiFS and Merged K_d490 images (July-2002 and Sept-2008)

4.2. IOP and SPM estimation

This section shows the results of IOP model application for calculation of absorption and backscattering coefficients (equations 8 to 11) and their relationship with SPM. IOP were computed directly from in situ data and then computed on MODIS, SeaWiFS and Merged images.

As the present study is focused on calculating SPM concentration, backscattering is considered purely from particular matter and absorption from pigments. It is based on that assumption that SPM do not

absorb. However, here is showed the relationship between SPM and both absorption and backscattering without go deep in how absorption is affected by SPM.

Figure 9 is showing the absorption coefficient estimated for *in situ* data compared to SPM and fluorescence. Here was evident that most wavelength fitted significantly well an exponential function, same as suggest Babin et al.(2003b).

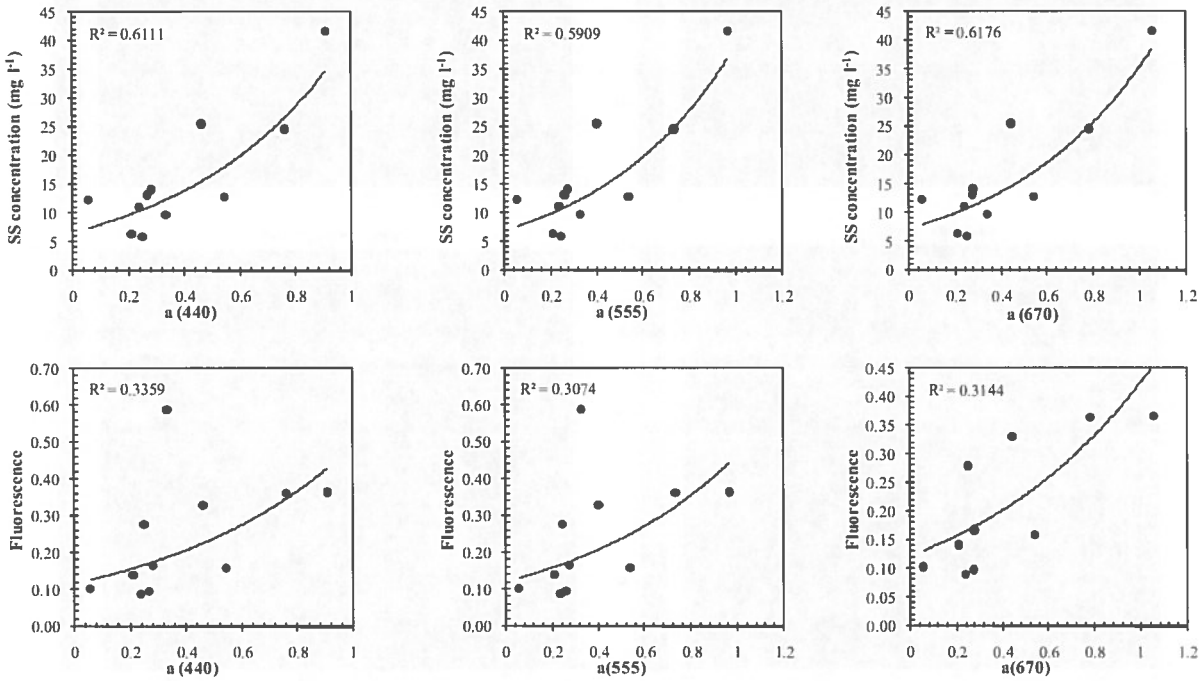

Figure 9 Comparison of absorption coefficient with SPM and Fluorescence at 440, 555 and 670 nm

In terms of backscattering coefficient estimation, the wavelength 555 nm is considering as the minimal absorption by particulate matter, thus it is selected for an overall examination of the relationship between scattering and particular matter concentration (Babin et al., 2003a). In this case linear relationship is applied to *in situ* data showing higher correlation coefficient for 555 nm.

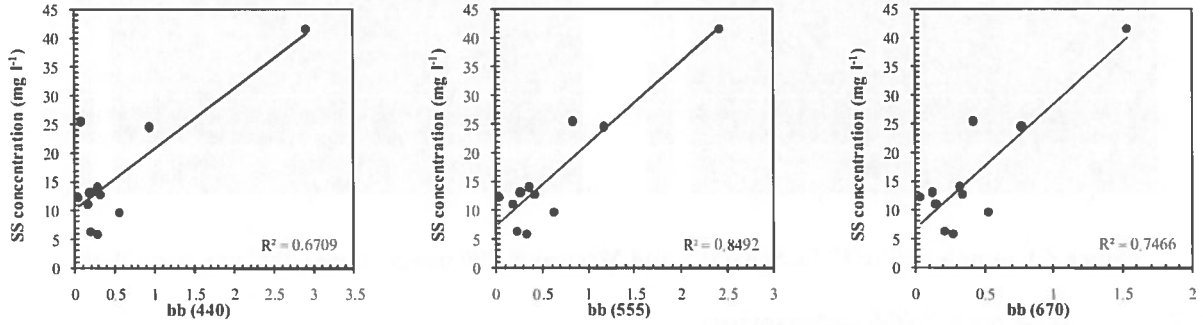

Figure 10 Comparison of backscattering coefficients with. SPM concentrations at 440, 555 and 670 nm)

Therefore, from relations above, were tested models for SPM from absorption and backscattering as following:

$$SPM(b_b) = 13.797 * (b_b 555) + 9.5174 \quad (17)$$

$$SPM(a) = 8.1018 * e^{1.8469 * a440} \quad (18)$$

Validation of SPM estimated from IOP model, was made using in situ measurements (whole calculation in Appendix D). From backscattering model the relative error is lower than absorption coefficient model (Table 7). However, correlation coefficient R^2 is better for *a(440)* than $b_b(550)$. This error analysis is showing that in general both models are underestimating SPM concentrations values in relation with *in situ* data. Backscattering (b_b) model shows RSME of 5.2 mg l^{-1} while absorption model (a) of 6.7 mg l^{-1}.

Table 7 Validation of SPM model (validation data set)

	SPM from a(440)	SPM from bb(555)
MAE	46.031	27.701
RMSE	6.785	5.263
Mean relative error (%)	-56.913	-49.260
Correlation	0.942	0.852

As well, error estimation was done using concentrations of SPM from INVEMAR water quality database REDCAM. This data base contains concentration of SPM from 2000 along the coastal line in not fix locations and with gaps in some years. It was selected 10 locations from different years between 2000 and 2007 completing a data set of 46 points (stations location in Figure 2).

In order to understand the associate errors of SPM estimation, points were classified in three groups according to the measured SPM concentration values (Table 8). Error analysis shows that the model is estimating the SPM concentrations with an accuracy of ± 3.3 mg l^{-1} for clear and relative turbid water (< 26 mg l^{-1}). In addition, an increment of errors is evident with more turbid waters (group 2 and 3) where seems that the model is underestimating approximately half of concentration that was measured. However, highest errors showed in the mouth of the rivers (group 3) probably are because the dynamic of river plume at moment of taking the samples. In general, the underestimation might be related to averaging of monthly data from the images.

Table 8 SPM Error analysis

	Group1	Group2	Group3
	(SPM < 26 mg l^{-1})	(26 mg l^{-1} < SPM < 56 mg l^{-1})	(SPM > 56 mg l^{-1})
MAE	11.38331	461.29297	13381.71908
RMSE	3.37392	21.47773	115.67938
Mean relative error (%)	-2.98320	131.0827021	397.46831
Correlation	0.48	0.35	0.15

Figure 11 is presenting an example of SPM map series from January to December 2007.

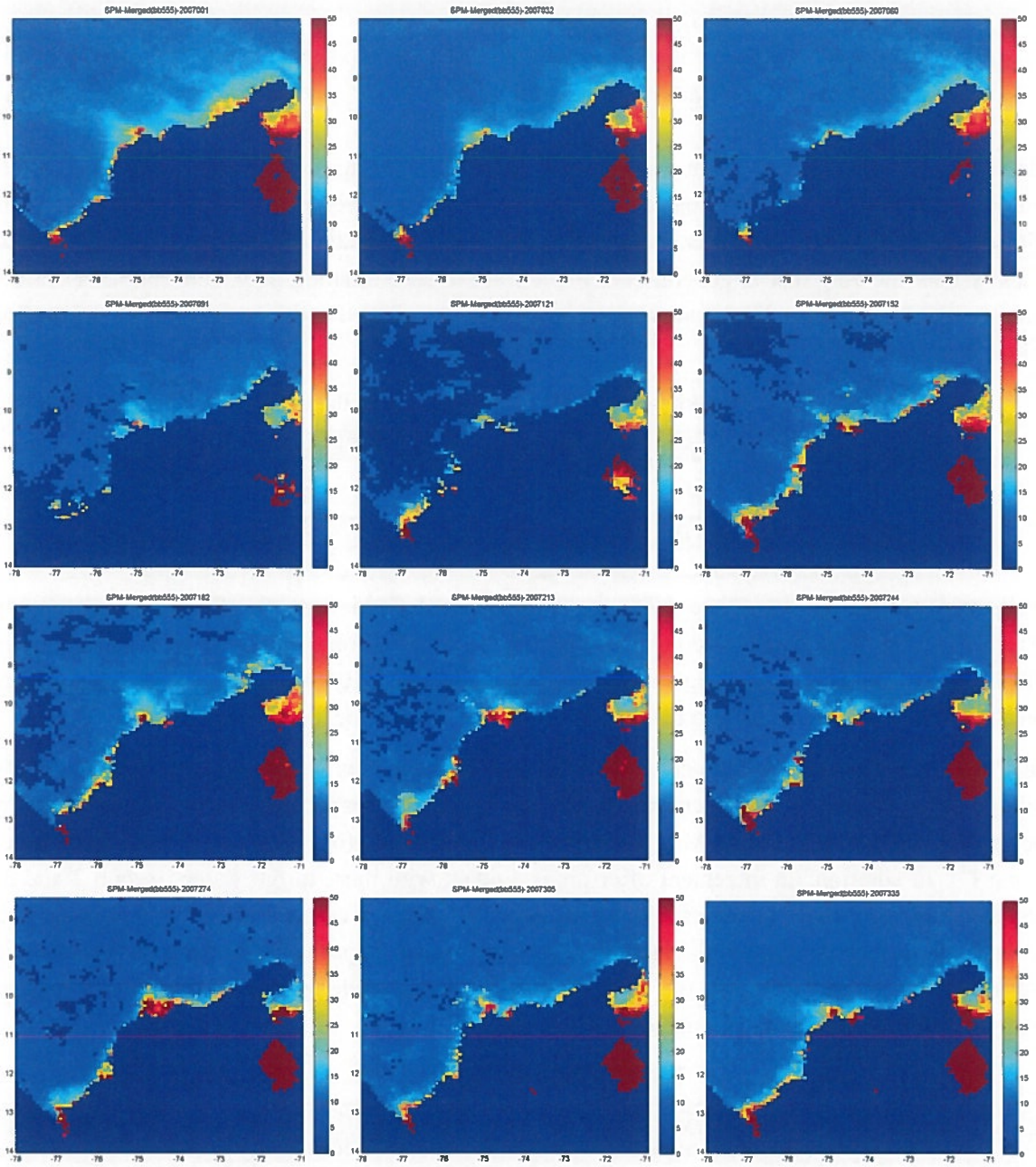

Figure 11 Maps of monthly SPM (mg l^{-1}) for 2007

4.3. Time series analysis

Analysis of time series was made using the averaging in scale to understand fluctuations of time series of SPM using variance average. For this exercise it was analyzed SPM concentration from 1998 to 2008 using the same 9 matchups for validation: 3 points in front of Sinú River, 4 points near of Magdalena river mouth and 2 points on Rosario Islands waters.

The purpose of this analysis was to understand if there is correlation between events presents in these three locations, particularly SMP fluctuations in the coral reef waters and high turbidity events in mouth of the rivers. Figure 12 shows variance averages fluctuation between 1998 and 2008 for the nine points.

In general, between 1999-2000 and 2002-2003 there are picks of high turbidity events for the points located in the mouth of the rivers. One of the most interesting finding here is a delay fluctuation patterns in Rosario Island in 2003-2004, which probably come out from those major turbidity events in the rivers in 2002-2003. Other interesting aspect is a kind of accumulation pattern in Rosario Islands which is showing a pick in 2008. It is probably due to small turbidity events occurred in both Rivers during 2004-2007.

Nevertheless, this kind of analysis needs more inquire in order to define quantitatively the fluctuation and periodicity of variation, which is out of the scope of this research. But indeed, this tool promise to be useful in monitoring programs and adaptation strategies.

Complete output graphs for four locations in Magdalena and Sinú Rivers other in Rosario Islands are in Appendix E.

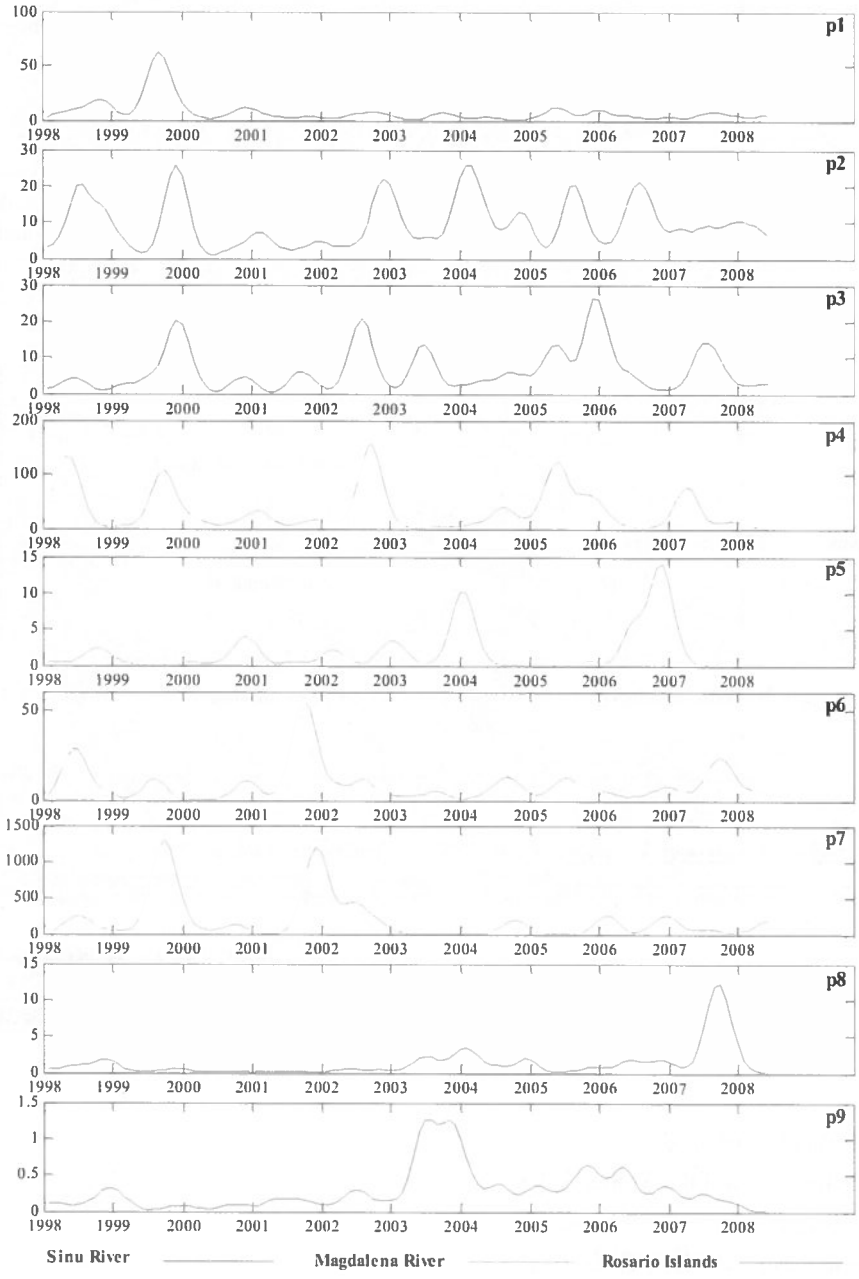

Figure 12 Scaled Average of SPM for 1998-2008 (9 points)

4.4. Code development

The algorithm was implemented in a new computer code using Matlab v. 7.6.0 (R2008a). The method is operational in the sense that it automatically provides the values of diffuse attenuation coefficient using ocean color radiometric data from MODIS, SeaWiFS or their merged products (Figure 13). In turn, these operational products are used to derive the absorption and backscattering coefficients and their relation with SPM concentrations (Figure 14). Additional tools were implemented for both modules to create image animation and for wavelet time series analysis.

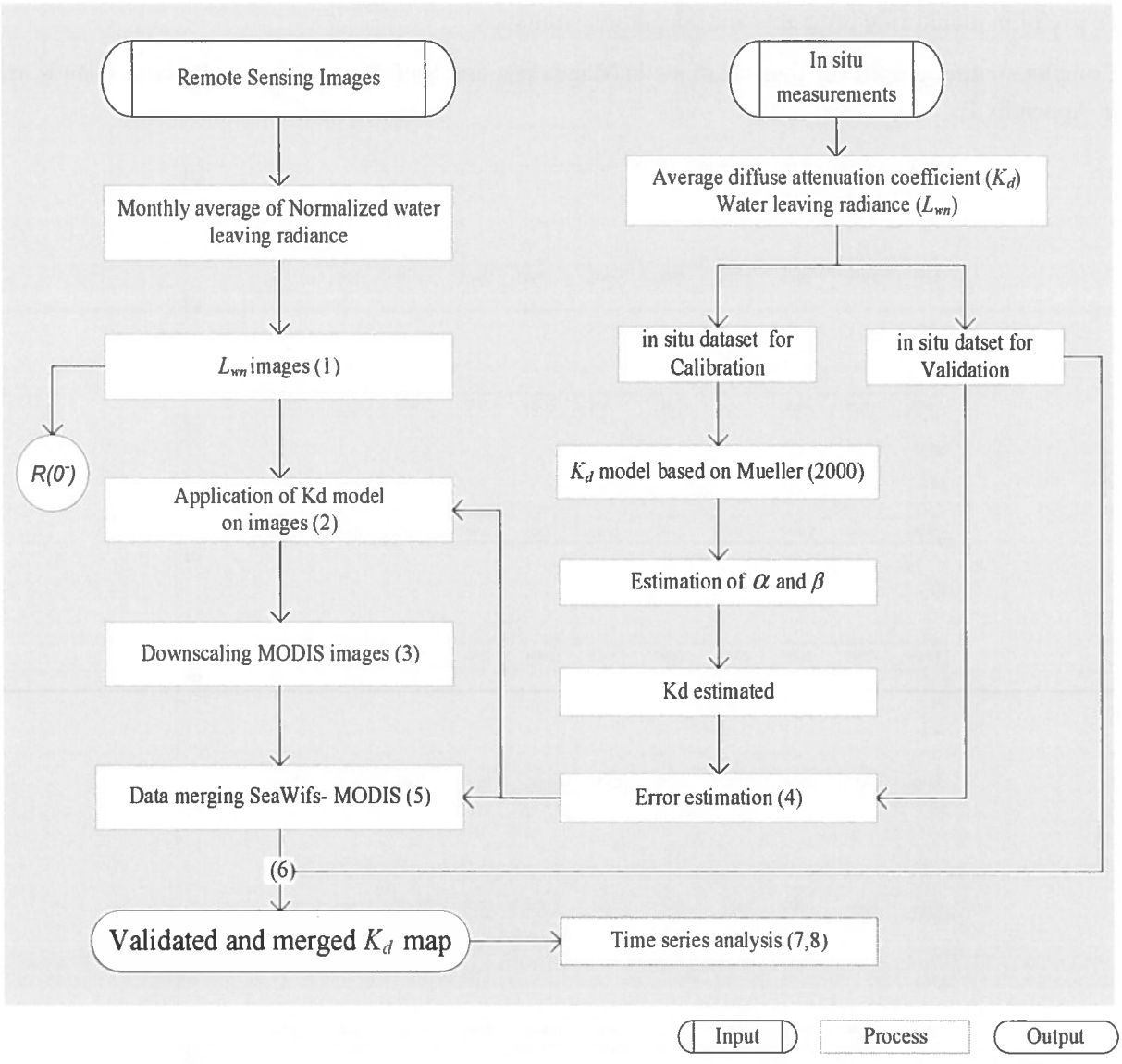

Figure 13 Sequence diagram for K_d and Merging

List of scripts:

1. Monthly average of L_{WN}
2. K_d computation MODIS & SeaWiFS
3. Downscaling K_d & L_{WN} 555 MODIS
4. Array time series MODIS & SeaWiFS
5. Merging L_{WN} 555 & K_d 490
6. Image animation K_d from MODIS, SeaWiFS and merged product

7. Array time series K_d merged
8. Wavelet analysis adapted from Torrence and Compo (1998)

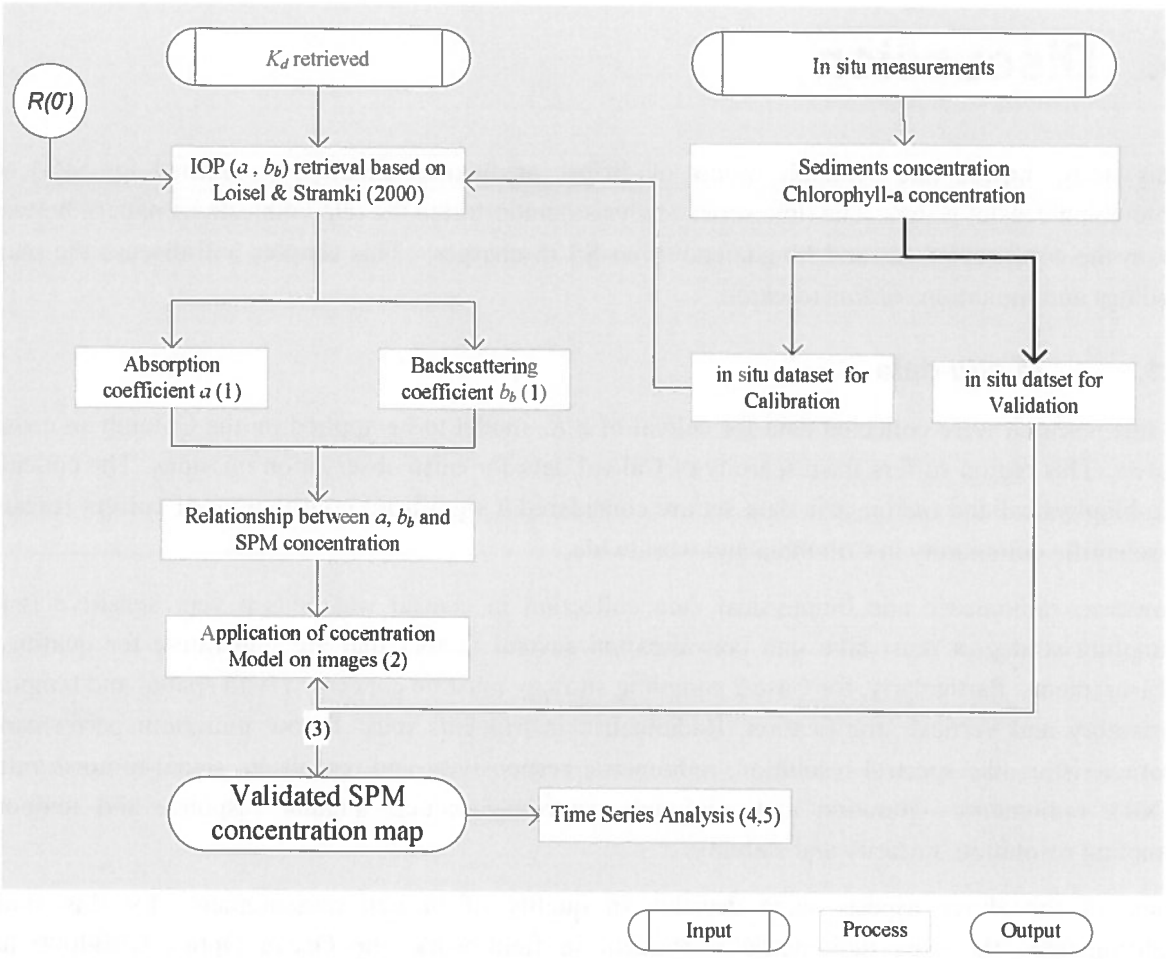

Figure 14 Sequence diagram for IOP & SPM

List of scripts:

1. Absorption and backscattering computation MODIS, SeaWiFS and merged product
2. SPM estimation MODIS, SeaWiFS and merged product
3. Image animation SPM MODIS, SeaWiFS and merged product
4. Array time series SPM MODIS, SeaWiFS and merged product
5. Wavelet analysis adapted from Torrence and Compo (1998)

5. Discussion

This study showed that available model of diffuse attenuation should be modified for SPM and Colombian coastal waters. The time series analysis demonstrated the tele-connections pattern between SS in the coral reef areas and Magdalene /Sinú SS discharges. This chapter will discuss the major findings and limitations of this research.

5.1. *In situ* data

In this research were collected data for cal/val of a K_d model to be applied on the Colombian coastal waters. This region suffers from scarcity of Cal/val data for earth observation missions. The collected geo-biophysical and radiometric data set are considered a significant contribution of current research to scientific community in Colombia and worldwide.

However, radiometric and biophysical data collection in coastal waters is a very sensitive issue. Sampling strategies must take into consideration several factors that are imperative for quality of measurements. Particularly, for Case 2 sampling strategy must be concerned with spatial and temporal variability and vertical stratification. Radiometric instruments must follow minimum performance characteristics like spectral resolution, radiometric responsivity and resolution, signal-to-noise ratios (SNR), radiometric saturation and minimum detectable values, angular response and temporal sampling resolution, linearity and stability.

Some of the above aspects were decisive in quality of *in situ* measurements for this study. Unfortunately, the used radiometric instrument in field work, the Ocean Optics USB4000 had saturation problems for irradiance and water leaving reflectance measurements causing rejection of more than 50% of measurements.

Other factors influenced quality of *in situ* data were the weather conditions that caused constant dynamic of plume of the rivers, mainly in Magdalena river mouth. In fact, field work has been done at the end of September, on wet season when high rainfalls are more intense and frequent.

Another inconvenient of sampling strategy was for Chl-a concentration measurement, which were mostly under threshold values making impossible to build calibration curve with fluorescence values. Here is important to observe that number of samples was small (only 10) and strategy sampling was not ideal due to complexity of transporting and processing samples at INVEMAR laboratory.

In spite of all theses difficulties, it was possible to build a radiometric and biophysical database with 11 points that facilitated calibration and validation processes. However, for future campaigns, more attention should be paid to the reliability, performance and calibration of radiometric instruments. Ideally, more samples should be taken in different seasons and water types.

5.2. Diffuse attenuation coefficient model

The empirical ratio model proposed by this research was partially validated with *in situ* data set and then compared with models of Mueller (2000) and Berthon et al (2002).

Mueller's model is originally developed to estimate K_d global product based on SeaWiFS water leaving radiances at 490 and 555 nm. Essentially calibration and validation of the method were using Case 1 waters. This means that SeaWiFS K_d490 data with values > 0.25 m^{-1} must be handled with caution. Our K_d values are varying between 0.07 and 2.1 m^{-1}. In fact this large variation necessitates new calibration of the K_d model, i.e. finding new coefficients (α and β) for the study area.

One adaptation of Mueller's model is Berthon's approach, which is considered alternative more suitable for coastal waters. If we compare coefficients α and β among the three models (see Table 5), Mueller has lowest values while Berthon's shows an increase in exponential and scope coefficients. Coefficients of current proposal are the highest, which might represent further sensitivity in the ratio model for turbid waters.

Our error analysis showed a good correlation between the three models. The R^2 value is larger than 0.98 for the three models. However, the values of the mean relative error were less than 1.5% for our model and exceeding 58% and 44% for Mueller and for Berthon model respectively.

The above results show that the developed K_d490 model is more representative of light attenuation processes in the area than the other two discussed models.

Recent developments of ocean color focus on merging spatial and spectral information in order to overcome limitation such as gaps between swaths, sun glint and cloud cover. In this work, we merged K_d products using weighted averaging. The weights were estimated from the error in derived products and model's uncertainty.

In general, there is an evident improvement in the merged products. However in terms of RMSE, the K_d merged product has higher error (0.291) than SeaWiFS which actually has the lower error among the three (0.277). This larger error of merged values is probably due to the spectral shift in ratio K_d490 model. This model was originally developed for SeaWiFS spectral bands. With respect to MODIS, there is a spectral difference (555 for SeaWiFS and 551 for MODIS) that might cause such variation. The differences in derived products from both sensors was reported by many studies (e.g. Darecki and Stramski, 2004; Patissier et al., 2004). Some study has suggested spectral data merging (Maritorena and Siegel, 2005b).

Besides the improvement in terms of relative errors after merging, there was an evident benefit related to cloud cover areas and missing data. In fact, this kind of advantage is the aim of the merging process, an improvement in the coverage in space and time exploiting redundancy in coincident ocean color missions (Gregg and Woodward, 1998).

5.3. IOP and SPM

The applied IOP model considers absorption and backscattering as total and does not decompose them into their different components: pigments, SPM and CDOM. Since main aim of this research is to retrieve SPM concentration, we made some considerations about backscattering and absorption coefficients.

Backscattering is considered only from particular matter. The 555 wavelength was chosen because this wavelength correspond to the minimal absorption by particular matter and is low impacted by

absorption of green pigments (Kirk, 1994; Mobley, 1994). For simplicity is assumed that SPM are mineral and clay origin and CDOM and chlorophyll, are not affecting the backscattering at this specific band. This assumption is however a crud simplification because CDOM and SPM have considerable influence at this spectral region. Also, measurement of CDOM and SPM absorption in this study area are not available.

Moreover, SPM model based on absorption at 440 nm was tested. The model uses the exponential fit found by others studies (e.g. Bowers et al., 1996; Kratzer et al., 2000). In spite of this relationship, is assumed that SPM do not absorb. There are evidences that absorption of SPM might help to understand the diversity of SPM spectral signature (Babin et al., 2003b). This approach would help to overcome the mixed spectral response of water constituents in Case 2 waters.

The strong relationship showed between SPM and absorption coefficient which should be considered in future research.

Validation of SPM model with REDCAM database showed that the model provided good estimates of SPM with accuracy of ±3.3 mg l^{-1} for waters with SPM concentration below 26 mg l^{-1} and up to ±115 mg l^{-1} for rivers mouths with SPM above 56 mg l^{-1}.

This high error could be explained by:

- Temporal and spatial averaging of L_{WN} is a generalization of one pixel of 4 x 4 km in the field represents an area between 1- 10 m. According to Mueller (2003), in Case 2 waters, pigment concentration derived from spatially averaged satellite radiance data will systematically underestimate the true spatial average concentration by as much as a factor of 2 when sub-pixel variability is significant.
- Particularly in Magdalena river mouth, the REDCAM database has a long variation in SPM measurements (26 to 600 mg l^{-1}) that can be influencing the error quantity.
- Considered threshold of SPM concentration, since saturation problems in radiometric measurements resulted in exclusion of some points with the highest SPM concentration values.
- Finally, spatial and temporal variability of the plume in sampling time.

Regarding to SPM time series analysis, the average scale analysis has revealed very interesting results. It has shown some fluctuation patterns in Rosario Island in 2003, can be related with specific high turbid events in Magdalena and Sinú River in 2002.

One of the most interesting finding was the time-lag fluctuation patterns in Rosario Islands. This time lag is most likely related to climate conditions and local / global circulation pattern. Is probably that these fluctuation would be related with El Niño phenomena. Effects of El Niño on Colombia have been reported for coincident periods of peak turbidity, 1998-1999, 2002-2003 and 2006-2007. Main effect in these periods is the increase in rainfall intensity about 20-30% of regular values.

Other important factor for determining the degradation risk of marine ecosystem is the level of exposure, environmental indicator defined as concentration and duration of the terrestrial flux into reef system. Somehow, results of time series analysis might be used as input for coral reef monitoring and promise to be useful for monitoring marine ecosystems and ultimately contributing to adaptation strategies of climate and human-induced environmental changes.

5.4. Limitations

Errors are originated from uncertainty in the measurements and introduced assumptions. Large errors in derived products are limiting factors to the applicability of any developed model. In this section we discuss the limitations in the context of *in situ* measurements, satellite measurements uncertainties and introduced assumptions.

Some of these limitations could be avoided with additional *in situ* measurements.

- Main limitation of this model is due to the limited number of calibration/ validation sites. The model should further be improved taking more measurements in very turbid waters and during dry season.
- The difference in satellite pixel size and point measurements is another source of uncertainty. Matchup field data usually characterize an area of around 1-10 m^2 while the satellite spatial scale is 4 kilometers. This environment mismatch in scales introduces an uncertainty that is often hard to quantify (IOCCG, 2006)
- Many steps are integrating the whole modeling process; each potentially produces an error that is propagated to the second step. Some of these errors were calculated: K_d model (RMSE = 0.154 m^{-1}), K_d merged images (RMSE = 0.291 m^{-1}), SPM model (RMSE = 5.26 mg l^{-1}). Nevertheless, another errors were unfeasible to estimate, for instance for irradiance reflectance $R(0^-)$, a and b_b and SeaWiFS L_{WN} 555 estimation.
- Model is assuming generalization by monthly L_{WN} average and MODIS downscaling averaging that as well are sources of uncertainties.
- Finally the model is considering three main assumptions, vertical and horizontal homogeneity, spectral independency and constant error for all radiometric quantities.

6. Conclusions and recommendations

6.1. Conclusions

- Biophysical and radiometric measurements data set for Case 2 waters in Colombia can contribute to the on going validation calibration efforts of ocean color products.
- The standard K_d model should be adapted form the Colombian waters. The modified model in this study succeeded in deriving good estimates of K_d from ocean color ratio with R^2 above 0.98 and RMSE of 0.154 m^{-1}. In comparison with others K_d490 models present model has better performance.
- Merged K_d products from SeaWiFS and MODIS has improved accuracy of K_d with mean relative error less than 2.1%. A second advantage of the merging is filling the missing data due to cloud cover
- Validation of SPM using external measurements (the REDCAM database) has shown that model estimates SPM with an accuracy of ±3.3 mg l^{-1} for waters with concentration below 26 mg l^{-1}. However model underestimates SPM concentrations in the rivers mouths (SPM > 56 mg l^{-1}) with an RMSE ±115 mg l^{-1}.
- Validation of SPM using external measurements (the REDCAM database) has shown that model estimates SPM with an accuracy of ±3.3 mg l^{-1} for waters with concentration below 26 mg l^{-1}. However model underestimates SPM concentrations in the rivers mouths (SPM > 56 mg l^{-1}) with an RMSE ±115 mg l^{-1}.
- Limitations of the model are related to amount *in situ* measurements for calibration/validation, size of pixels and local heterogeneity, intrinsic uncertainties in ocean Level 2 products, uncertainties propagation, monthly L_{WN} average and MODIS downscaling averaging.
- The model provided maps of SPM concentrations that facilitate monitoring of the temporal and spatial variations of the suspended sediment that might be use to evaluate its effects on marine ecosystem in the study area.
- SPM time series analysis for period 1998-2008 showed some fluctuation patterns in Rosario Island that can be related to specific turbid events in Magdalena and Sinú River. This information promise to be useful for monitoring marine ecosystems and contributing to adaptation strategies in the face of human induced environmental changes.
- The methodology was implemented in a new computer code for the study area and is operational in the sense that it automatically provides the values of diffuse attenuation coefficient at 490 nm, IOP (a and b_b) and SPM using ocean color radiometric data from SeaWiFS, MODIS or merged products.

6.2. Recommendations

- More radiometric and biophysical measurements should be taken in high turbid waters and during dry season. Sampling data will improve model performance making more realistic SPM concentration values mostly in rivers mouth areas.
- Sampling strategies should follow carefully technical specifications and standard calibration in order to avoid instrumental errors in field measurements. In this way wrong data and uncertainties due to *in situ* measurements will be reduced.
- Spectral and spatial data merging using MERIS images would help to improve optical information of water constituents in turbid tropical waters. Using more spatial resolution uncertainties due to size of pixels and local heterogeneity will be reduced. As well, more spectral information will help to understand the satellite spectral signature of SPM.
- More understanding of relationship between SPM and absorption coefficient would help to improve the knowledge trends and variability of particles in Case 2 waters. Moreover, it will help to differentiate SMP from the other water constituents, mostly CDOM that has similar signature.
- Uncertainties budget estimation would benefit quantification of associate errors in ocean optic modeling. Mostly those that are assumed know or insignificant such as *in situ* data uncertainties or pixel size and local heterogeneity.
- Using techniques of tele-connections and identifying persistent patterns in order to increase the knowledge of effect of climate change on the water quality
- Connection between earth observation products and marine ecosystems will facilitate monitoring of coral reefs through extraction of health indicators.

7. References

Andrade, C.A., 1995. Variabilidad anual del contenido de carbon organico en la superficie del Caribe occidental desde CZCS (Annual variability of organic carbon content at the western Caribbean sea surface from CZCS). Boletín Científico CIOH, 16: 15-24.

Andrade, C.A. and Barton, E.D., 2005. The Guajira upwelling system. Continental Shelf Research, 25(9): 1003-1022.

Andrade, C.A., Bernal, G., Ricaurte, C., Mayo, G., Domínguez, J., Orejarena, J., Gutiérrez, A. and Castro, W., 2005. Estudio oceanográfico de los bancos de Salmedina, Caribe colombiano. Escuela Naval Almirante Padilla, Cartagena, A.G. Editores, Bogota.

Babin, M., Morel, A., Fournier-Sicre, V., Fell, F. and Stramski, D., 2003a. Light scattering properties of marine particles in coastal and open ocean waters as related to the particle mass concentration. Limnology and Oceanography, 48(2): 843-859.

Babin, M., Stramski, D., Ferrari, G.M., Claustre, H., Bricaud, A., Obolensky, G. and Hoepffner, N., 2003b. Variations in the light absorption coefficientes of phytoplanckton, nonalgal particles, and dissolved organic matter in coastal water around Europe. Journal of Geophysical Research, 108(C7): 1-20.

Bernal, G., Velásquez, A., Vargas, I., Agudelo, A.C., Andrade, C.A., Domínguez, J.G., Ricaurte, C. and Mayo, G., 2006. Variabilidad de los aportes a los sedimentos superficiales durante un ciclo anual en los Bancos de Salmedina. Boletín de Investigaciones Marinas y Costeras, 35: 59-75.

Berthon, J.-F., Zibordi, G., Doyle, J.P., Grossi, S., van der Linde, D. and Targa, C., 2002. Coastal Atmosphere and Sea Time Series (CoASTS): Data Analysis. In S. B. Hooker, & E. R. Firestone (Eds.), NASA-GSFC, Greenbelt, Maryland.

Binding, C.E., Bowers, D.G. and Mitchelson-Jacob, E.G., 2003. An algorithm for the retrieval of suspended sediment concentrations in the Irish Sea from SeaWiFS ocean colour satellite imagery. International Journal of Remote Sensing, 24(19): 3791 - 3806.

Bowers, D.G., Harker, G.E.L. and Stephan, B., 1996. Absorption spectra of inorganic particles in the Irish Sea and their relevance to remote sensing of chlorophyll. International Journal of Remote Sensing, 17(12): 2449-2460.

Cañon, M.L. and Santamaria del Angel, E., 2003. Influencia de la pluma del río Magdalena en el Caribe colombiano. Boletín Científico CIOH, 21: 66-84.

Clark, D.K., Baker, E.T. and Strong, A.E., 1980. Upwelled spectral radiance distribution in relation to particulate matter in sea water. Boundary-Layer Meteorology, 18(3): 287-298.

Darecki, M. and Stramski, D., 2004. An evaluation of MODIS and SeaWiFS bio-optical algorithms in the Baltic Sea. Remote Sensing of Environment, 89(3): 326-350.

Diaz, J.M., Barrios, L.M., Cendales, J., Garzón-Ferreira, J., Geister, J., López-Vitoria, M., Ospina, G.H., Parra, F., Pinzón, J., Vargas, B. and Zapata, F.A., 2000. Áreas coralinas de Colombia. Series de publicaciones especiales, v. 5. INVEMAR, Santa Marta, 97 pp.

Doerffer, R., Fischer, J., Stössel, M., Brockmann, C. and Grassl, H., 1989. Analysis of thematic mapper data for studying the suspended matter distribution in the coastal area of the German Bight (North Sea). Remote Sensing of Environment, 28: 61-73.

Froidefond, J.M., Castaing, P., Jouanneau, J.M., Prud'Homme, R. and Dinet, A., 1993. Method for the quantification of suspended sediments from AVHRR NOAA-11 satellite data. International Journal of Remote Sensing, 14(5): 885-894.

Garay, J., Marín, B., Ramírez, G., Troncoso, W., Velez, A., Calvano, N., Medina, O., Lozano, H., Cadavid, B., Acosta, J., Lamcheros, A. and Rondon, A., 2001. Diagnóstico y evaluación de la calidad ambiental marina en el Caribe y Pacífico colombiano. Red de vigilancia para la protección y conservación de la calidad de lasaguas marinas y costeras. Infome final. Tomo II. 260 p.

Garay, J., Ramírez, G., Betancourt, J., Marín, B., Cadavid, B., Panizzo, L., Lesmes, J., Sánchez, H. and Franco, A., 2003. Manual de técnicas analíticas para la determinación de parámetros fisicoquímicos y contaminantes marinos: aguas, sedimentos y organismos, Serie de documentos Generales No. 13. INVEMAR, Santa Marta, 177 pp.

Gordon, H.R. and Clark, D.K., 1981. Clear water radiances for atmospheric correction of coastal zone color scanner imagery. Applied Optics, 20: 4175-4180.

Gordon, H.R. and Morel, A., 1983. Remote assessment of ocean color for interpretation of satellite visible imagery, a review. In Lecture notes on coastal and estuarine studies. Springer-Verlag, New York.

Gordon, H.R. and Wang, M.H., 1994. Retrieval of water-leaving radiance and aerosol aoptical-thickness over the oceans with seawifs - a preliminary algorithm. Applied Optics, 33(3): 443-452.

Gregg, W.W. and Woodward, R.H., 1998. Improvements in coverage frequency of ocean color: Combining data form SeaWiFS and MODIS. IEEE Transactions on Geoscience and Remote Sensing, 36: 1350-1353.

INVEMAR, 2003. Programa holandés de asistencia para estudios de cambio climático, Colombia: Definición de la vulnerabilidad de los sistemas biogeofísicos y socioeconómicos debido a un cambio en el nivel del mar en la zona costera colombiana (Caribe continental, Caribe insular y Pacifico) y medidas para su adaptación. VII Tomos. Resumen Ejecutivo y CD-Atlas digital. Programa de Investigación para la Gestión Marina y Costera-GEZ, Santa Marta, Colombia.

INVEMAR, 2008. Digital Cartography, Marine and Costal Information System. In: LabSI (Editor), Santa Marta.

IOCCG, 2006. Remote Sensing of Inherent Optical Properties: Fundamentals, Tests of Algorithms, and Applications. Lee, Z.-P. (ed), Reports of the International Ocean-Colour Coordinating Group, No. 5, IOCCG, Darthmouth, Canada.

IOCCG, 2008. International Ocean Colour Coordinating Group. Online web page; URL: http://www.ioccg.org/. Access date: 15-Oct-2008.

Kirk, J.T.O., 1994. Light & photosynthesis in aquatic ecosystems. Cambridge University Press, Cambridge.

Kratzer, S., Bowers, D. and Tett, P.B., 2000. Seasonal changes in colour ratios and optically active contituents in the optical Case-2 waters of the Menai Strait, North Wales. International Journal of Remote Sensing, 21(11): 2225 - 2246.

Kratzer, S., Brockmann, C. and Moore, G., 2008. Using MERIS full resolution data to monitor coastal waters. A case study from Himmerfjärden, a fjord-like bay in the northwestern Baltic Sea. Remote Sensing of Environment, 112(5): 2284-2300.

Lee, Z.-P., Carder, K., Mobley, C., Steward, R.G. and Patch, J.S., 1999. Hyperspectral remote sensing for shallow waters: 2. Deriving bottom depths and water properties by optimization Applied Optics, 38(18): 3831-3843.

Loisel, H., Nicolas, J., Deschamps, P. and Frouin, R., 2002. Seasonal and inter-annual variability of particulate organic matter in the global ocean. Geophysical Research Letters, 29.

Loisel, H. and Stramski, D., 2000. Estimation of the inherent optical properties of natural waters from the irradiance attenuation coefficient and reflectance in the presence of raman scattering. Applied Optics, 39(18): 3001-3011.

Lund-Hansen, L.C., 2004. Diffuse attenuation coefficients Kd(PAR) at the estuarine North Sea-Baltic Sea transition: time-series, partitioning, absorption, and scattering. Estuarine, Coastal and Shelf Science, 61(2): 251-259.

Maritorena, S. and Siegel, D.A., 2005a. Consistent merging of satellite ocean color data sets using a bio-optical model. Remote Sensing of Environment, 94: 429-440.

Maritorena, S. and Siegel, D.A., 2005b. Consistent merging of satellite ocean color data sets using a bio-optical model. Remote Sensing of Environment, 94(4): 429-440.

Mélin, F., Berthon, J.-F. and Zibordi, G., 2005. Assessment of apparent and inherent optical properties derived from SeaWiFS with field data. Remote Sensing of Environment, 97(4): 540-553.

Miller, R.L. and McKee, B.A., 2004. Using MODIS Terra 250 m imagery to map concentrations of total suspended matter in coastal waters. Remote Sensing of Environment, 93(1-2): 259-266.

Mishra, D.R., Narumalani, S., Rundquist, D. and Lawson, M., 2005. Characterizing the vertical diffuse attenuation coefficient for downwelling irradiance in coastal waters: Implications for water penetration by high resolution satellite data. ISPRS Journal of Photogrammetry and Remote Sensing, 60(1): 48-64.

Mobley, C.D., 1994. Light and water: radiative transfer in natural waters. Academic Press, San Diego, 579 pp.

Morel, A. and Gentili, B., 1993. Diffuse reflectance of oceanic waters. II Bidirectional aspects. Applied Optics, 32(33): 6864-6879.

Morel, A. and Mueller, J.L., 2003. Normalized water-leaving radiance and remote sensing reflectance: bidirectional reflectance and other factors. In: J.L. Mueller, R.W. Austin, A. Morel, G.S. Fargion and C.R. McClain (Editors), Ocean optics protocols for satellite ocean color sensor validation, Revision 4, Volume III, NASA/TM-2003-21621. NASA Goddard Space Flight Space Center, Greenbelt, Maryland.

Mueller, J.L., 2000. SeaWiFS algorithm for the diffuse attenuation coefficient K(490) using water leaving radiances at 490 and 555 nm., Greenbelt, Maryland: NASA-GSFC.

Mueller, J.L., 2003. Field measurements, sampling strategies, ancillary data, metadata, and data archival: general protocols. In: J.L. Mueller, R.W. Austin, A. Morel, G.S. Fargion and C.R. McClain (Editors), Ocean optics protocols for satellite ocean color sensor validation, Revision 4, Volume III, NASA/TM-2003-21621. NASA Goddard Space Flight Space Center, Greenbelt, Maryland.

Mumby, P.J., Skirving, W., Strong, A.E., Hardy, J.T., LeDrew, E.F., Hochberg, E.J., Stumpf, R.P. and David, L.T., 2004. Remote sensing of coral reefs and their physical environment. Marine Pollution Bulletin, 48(3-4): 219-228.

NASA, 2009. Ocean Color WEB. Online web page; URL: http://oceancolor.gsfc.nasa.gov/. Access date: 20-Jan-2009.

Patissier, D.B., Tilstone, G.H., Martinez-Vicente, V. and Moore, G., 2004. Comparison of bio-physical marine products from SeaWiFS, MODIS and bio-optical model with in situ measurements from Northern European waters. Journal of Optics A: Pure and Applied Optics, 6: 875-889.

Pottier, C., Garcon, V., Larnicol, G., Sudre, J., Schaeffer, P. and Le Traon, P.-Y., 2006. Merging SeaWiFS and MODIS/Aqua ocean color data in north and equatorial Atlantic using weighted averaging and objective analysis. IEEE Transactions on Geoscience and Remote Sensing, 44(11): 3436-3451.

Restrepo, J.D. and Kjerfve, B., 2000. Magdalena river: interannual variability (1975-1995) and revised water discharge and sediment load estimates. Journal of Hydrology, 235(1-2): 137-149.

Restrepo, J.D. and López, S.A., 2008. Morphodynamics of the Pacific and Caribbean deltas of Colombia, South America. Journal of South American Earth Sciences, 25(1): 1-21.

Restrepo, J.D., Zapata, P., Diaz, J.A., Garzon-Ferreira, J. and Garcia, C.B., 2006. Fluvial fluxes into the Caribbean Sea and their impact on coastal ecosystems: The Magdalena River, Colombia. Global and Planetary Change, 50(1-2): 33-49.

Ruiz-Ochoa, M., Bernal, G. and Polania, J., 2008. Influencia del río Sinú y el Mar Caribe en el sistema lagunar de Cispatá. Boletín de Investigaciones Marinas y Costeras, 37(1): 31-51.

Segal, B., Evangelista, H., Kampel, M., Gonçalves, A.C., Polito, P.S. and dos Santos, E.A., 2008. Potential impacts of polar fronts on sedimentation processes at Abrolhos coral reef (South-West Atlantic Ocean/Brazil). Continental Shelf Research, 28(4-5): 533-544.

Smith, R.C. and Baker, K.S., 1978. Optical classification of natural waters. Limnology and Oceanography, 23: 260-267.

Stramski, D., 1999. Estimation of paticulate organic carbon in the ocean from satellite remote sensing. Science, 285: 239-242.

Tassan, S. and Sturm, R., 1986. An algorithm for the retrieval of sediment content in turbid coastal waters from CZCS data. International Journal of Remote Sensing, 7(5): 643 - 655.

Torrence, C. and Compo, G.P., 1998. A practical guide to wavelet analysis. Bulletin of the American Meteorological Society, 79(1): 61-78.

Udy, J., Gall, M., Longstaff, B., Moore, K., Roelfsema, C., Spooner, D.R. and Albert, S., 2005. Water quality monitoring: a combined approach to investigate gradients of change in the Great Barrier Reef, Australia. Marine Pollution Bulletin, 51(1-4): 224-238.

Warrick, J.A., Mertes, L.A.K., Siegel, D.A. and Mackenzie, C., 2004. Estimating suspended sediment concentrations in turbid coastal waters of the Santa Barbara Channel with SeaWiFS. International Journal of Remote Sensing, 25(10): 1995-2002.

8. Appendixes

Appendix A. Instruments and materials

The field work was fully supported by the Marine and Coastal Research Institute (INVEMAR). Radiometric instruments and materials were provided by ITC, CNRS, INVEMAR, and others designed by present research.

Instruments and materials

Name	Source
USB4000 Miniature Fiber Optic Spectrometer	CNRS
USB4000 Miniature Fiber Optic Spectrometer	ITC
LS-1-CAL Calibrated Tungsten Halogen Light Source	ITC
WS-1-SL White Reflectance Standard with Spectralon	ITC
CC3 Cosine corrector	ITC
Optical cable 400 micron, QP400-2-UV/BX	ITC
Aluminum arms	PLOZANO
Laptop Dell	INVEMAR
Laptop Toshiba	PLOZANO
Spectra suite (Software)	CNRS
Fluorometer (Turner)	ITC
USB cable	CNRS
Sounding line	INVEMAR
Refractometer	INVEMAR
Secchi disck	INVEMAR
GPS Garmin 76s	INVEMAR
Suction bomb	INVEMAR
Filtration set and plastic bottles	INVEMAR
Microfibre filters (GF/A, 47mm 1820 047) Whatman ® 1.6 µm	INVEMAR
Photo camera	CGARCIA
Electric adaptor and cables	PLOZANO
Car battery	PLOZANO
Battery recharger	INVEMAR
Transparent plastic bottles (500 ml)	INVEMAR
Black plastic bottles (2 litter)	INVEMAR
Acrylic tables	INVEMAR
Pens, Pencils, sticking plaster, plastic 2*2 m, silicon	PLOZANO

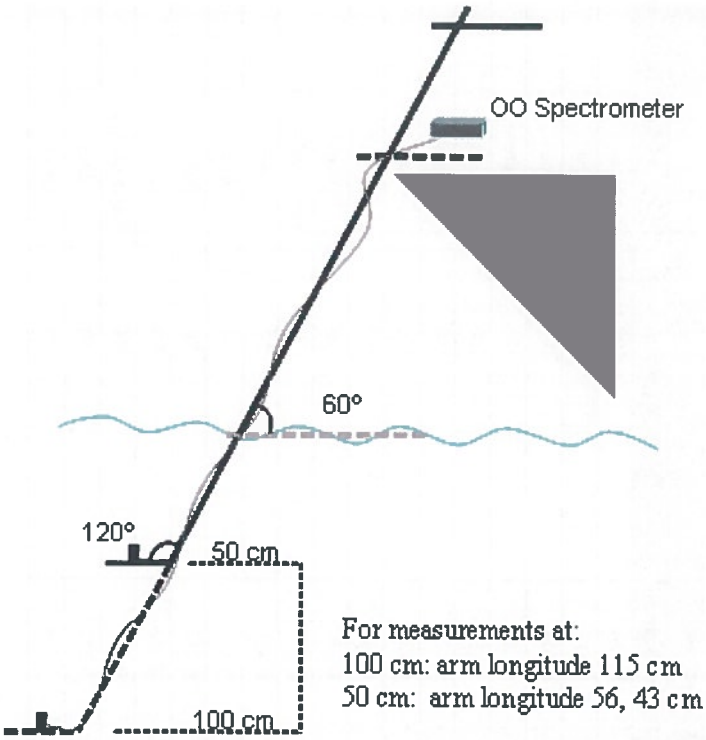

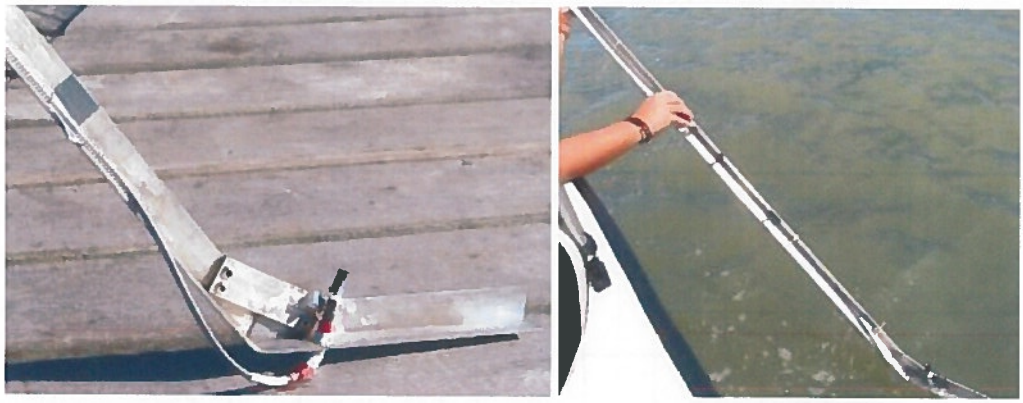

Aluminum arm design for underwater irradiance measurements

Appendix B. *In situ* measurements

SAMPLING RIO SINU: 20 -21 September 2008													
Station	**Longitude**	**Latitude**	**Date**	**time**	**Bottom depth**	**Transparency**	**Salinity**	**SS(mg l^{-1})**	**Fluorescence**	**Cl_a(mg l^{-1})**	**Cloud coverage**	**Watercolour**	**Exclusion criteria**
1	-75.989426	9.537365	09/20/08	10:59:08 am	42.5	12.8	33.5	0.413	0.150		100	Blue	1
2	-75.984382	9.529300	09/20/08	11:43:19 am	41.0	11.5	33.5	12.114	0.114		100	Blue	1
3	-75.980174	9.520895	09/20/08	12:11:11 pm	38.0	11.6	34.0	5.800	0.106		100	Blue	1
4	-75.976067	9.511358	09/20/08	12:52:03 pm	31.5	11.6	34.0	-1.403	0.142		100	Blue-green	1
5	-75.972729	9.503299	09/20/08	1:23:01 pm	22.6	12.6	34.0	2.204	0.111		100	Green	1
6	-75.969538	9.494377	09/20/08	1:50:21 pm	17.3	8.0	29.5	7.400	0.475		100	Green	1
7	-75.966762	9.486296	09/20/08	2:15:00 pm	13.5	7.5	20.0	4.409	0.936		100	Green	1
8	-75.962957	9.477398	09/20/08	2:37:12 pm	11.7	2.6	13.5	9.200	0.841		100	Green	1
9	-75.962757	9.468641	09/21/08	9:06:27 am	10.2	0.7	21.5	-1704.600	0.235		70	Green	3
10	-75.963941	9.456880	09/21/08	9:58:45 am	8.5	0.6	16.5	23.200	0.289		70	Green-yellow	4
11	-75.957986	9.448240	09/21/08	10:13:30 am	4.6	0.2	2.0	35.200	0.491		80	Green	5
12	-76.020366	9.495005	09/21/08	10:57:09 am	28.0	8.6	25.0	8.800	0.353		80	Green	5
13	-76.006135	9.481504	09/21/08	11:43:11 am	20.2	6.5	20.0	11.618	0.252		80	Green	5
14	-75.992958	9.468932	09/21/08	11:59:32 am	15.5	3.4	26.5	11.400	0.182		90	Green	5
15	-75.979790	9.456831	09/21/08	1:10:21 pm	11.1	1.2	14.5	15.600	0.305		100	Green-yellow	5
16	-75.934346	9.521443	09/21/08	1:55:31 pm	35.9	6.0	29.0	8.800	0.221		50	Green	5
17	-75.935283	9.502974	09/21/08	2:23:46 pm	22.3	7.0	29.0	9.000	0.250		20	Green	5

SAMPLING RIO MAGDALENA: 23 – 24 September 2008												
Station	**Longitude**	**Latitude**	**Date**	**time**	**Bottom depth**	**Transparency**	**Salinity**	**SS(mg l^{-1})**	**Fluorescence**	**Cl_a(mg l^{-1})**	**Cloud coverage**	**Watercolour**	**Exclusion criteria**
18	-74.946475	11.065558	09/23/08	9:42:00 am	14.6	10.0	34.5	6.400	0.142		40	Green	
19	-74.946431	11.056191	09/23/08	10:25:34 am	12.6	8.0	34.0	12.800	0.160		40	Green	
20	-74.945591	11.046745	09/23/08	10:49:41 am	11.4	7.0	32.5	14.200	0.168		50	Green	
21	-74.943768	11.036264	09/23/08	10:59:48 am	10.0	5.0	34.0	10.400	0.171		40	Green	4
22	-74.943944	11.026255	09/23/08	11:21:53 am	7.3	6.0	34.5	8.419	0.162		90	Green	4
23	-74.970022	10.994606	09/23/08	12:23:07 pm	5.9	5.0	35.0	8.000	0.138		90	Green	4
24	-74.857779	11.107117	09/24/08	9:34:28 am	7.1	0.0	1.5	164.671	0.561	0.10	20	Yellow	2
25	-74.861932	11.099662	09/24/08	9:45:08 am	7.1	0.5	11.5	25.600	0.331	0.10	30	Yellow	
26	-74.868502	11.093114	09/24/08	11:50:35 am	8.5	0.5	17.0	50.499	0.421	0.36	100	Green-yellow	2
27	-74.875377	11.087113	09/24/08	12:17:39 pm	9.8	3.0	25.0	9.800	0.590	3.09	100	Green	
28	-74.881734	11.080594	09/24/08	12:36:13 pm	8.8	5.0	33.5	33.200	0.309	0.44	100	Green	1
29	-74.885800	11.088402	09/24/08	1:16:10 pm	10.9	5.0	33.5	6.000	0.280	0.10	100	Green	
30	-74.885984	11.087899	09/24/08	1:37:05 pm	10.8	0.8	16.0	24.600	0.364	0.10	70	Green-yellow	
31	-74.880369	11.096236	09/24/08	2:06:47 pm	14.1	0.4	18.0	41.600	0.366	0.10	30	Yellow	
32	-74.874815	11.102732	09/24/08	2:23:57 pm	18.3	0.2	14.0	45.400	0.382	0.27	50	Yellow	3
33	-74.869010	11.109684	09/24/08	2:44:49 pm	66.9	0.1	10.5	73.200	0.465	0.10	50	Yellow	5

SAMPLING ROSARIO ISLAND 25 September 2008												
Station	**Longitude**	**Latitude**	**Date**	**time**	**Bottom depth**	**Transparency**	**Salinity**	**SS(mg l^{-1})**	**Fluorescence**	**Cl_a(mg l^{-1})**	**Cloud coverage**	**Watercolour**	**Exclusion criteria**
34	-75.737903	10.244681	09/25/08	12:00:53 pm	-	23.4	34.0	12.800	0.148		20	Green dark	5
35	-75.744062	10.251008	09/25/08	12:41:23 pm	-	23.5	34.0	10.200	0.118		20	Green dark	3
36	-75.751414	10.257109	09/25/08	12:49:33 pm	-	24.0	34.0	9.800	0.105		20	Green dark	3
37	-75.757637	10.263368	09/25/08	1:08:58 pm	-	23.0	32.5	38.600	0.092		5	Blue-green	5
38	-75.764314	10.269608	09/25/08	1:27:51 pm	-	25.0	33.5	13.200	0.099		10	Blue-green	
39	-75.769648	10.275602	09/25/08	1:52:26 pm	-	24.0	34.0	11.623	0.088		10	Blue-green	3
40	-75.776559	10.281798	09/25/08	2:12:15 pm	-	25.0	32.0	11.200	0.091		5	Blue-green	
41	-75.782335	10.288853	09/25/08	2:34:13 pm	-	24.0	31.5	38.400	0.108		5	Blue-green	3
42	-75.788472	10.294351	09/25/08	2:49:50 pm	-	24.0	33.0	40.600	0.098		0	Blue-green	3
43	-75.795120	10.300479	09/25/08	3:12:14 pm	-	24.0	33.0	12.400	0.104		0	Blue	

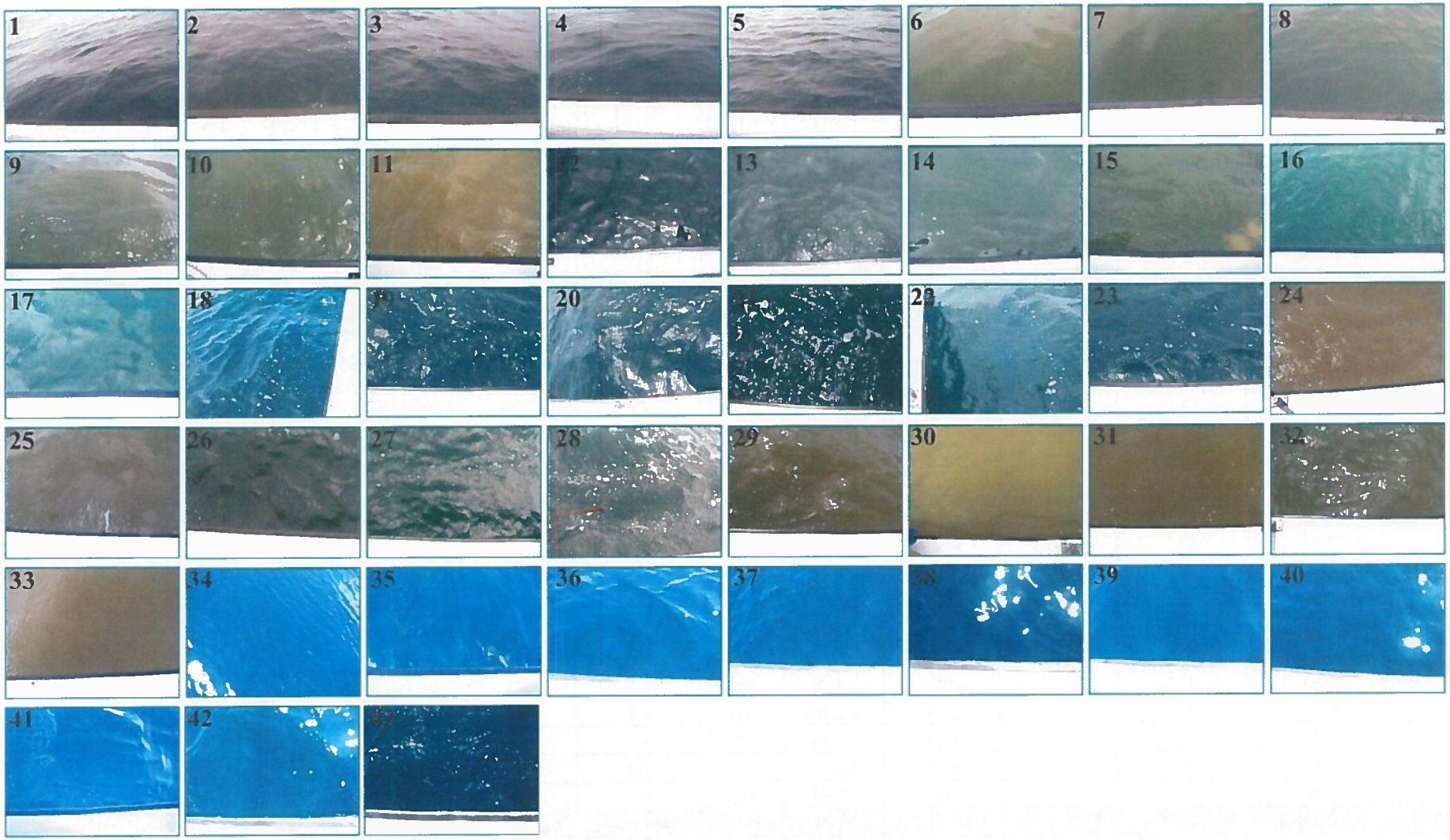

Water colour - pictures taken *in situ*

Appendix C. K_d model

Relative errors

Point location			K_d Sept MODIS	K_d Measured*	Error	Relative error %
Column	Row	Stations				
50	110	11	0.217	0.736	0.269	-70.471
48	109	12	0.272	0.357	0.007	-23.770
49	110	14,13,15	0.429	0.501	0.005	-14.448
50	109	16	0.357	0.399	0.002	-10.382
74	71	18	0.174	0.400	0.051	-56.510
74	72	19, 20	0.279	0.709	0.186	-60.721
76	71	25,31,27,29,30,26	NaN**	1.111	-	-
55	91	34,37	0.108	0.597	0.239	-81.949
54	91	38	0.097	0.356	0.067	-72.905
54	90	40,43	0.075	0.208	0.018	-63.835
						Mean Relative error %
				MSE K_d MODIS	0.094	-50.555
				RMSE	0.306	

Point location			K_d Sept SeaWiFS	K_d Measured	Error	Relative error %
Column	Row	Stations				
25	56	11,14,15	0.462	0.633	0.029	-26.960
25	55	12,13	0.399	0.349	0.002	14.331
26	55	16	0.412	0.399	0.000	3.330
38	36	18,19,20	0.740	0.606	0.018	22.144
39	36	25,26	2.043	1.419	0.390	44.033
38	36	27,29,30,31	0.740	0.957	0.047	-22.604
28	46	34,37,38,40	0.167	0.393	0.051	-57.448
						Mean Relative error %
				MSE K_d SeaWiFS	0.077	-3.311
				RMSE	0.277	

Point location			K_d Sept Merged	K_d Measured	Error	Relative errors %
Column	Row	Stations				
25	56	11,14,15	0.462	0.633	0.029	-26.960
25	55	12,13	0.420	0.349	0.005	20.577
26	55	16	0.424	0.399	0.001	6.458
38	36	18,19,20	0.740	0.606	0.018	22.144
39	36	25,26	2.043	1.419	0.390	44.033
38	36	27,29,30,31	0.740	0.957	0.047	-22.604
28	46	34,37,38,40	0.175	0.393	0.047	-55.364
						Mean Relative error %
				MSE K_d Merged	0.085	2.541
				RMSE	0.291	

* K_d Measured = average of K_d 490 values for number of stations located in 1 pixel; ** NaN= no data

Appendix D. IOP and SPM model

Sun zenith angle

Station	Longitude	Latitude	Date	Time	Sun zenith angle
18	-74.94647474	11.0655581	23/09/2008	9:40:00 a.m.	34.7147
19	-74.94643089	11.05619079	23/09/2008	10:20:00 a.m.	25.5452
20	-74.94559097	11.04674548	23/09/2008	10:37:00 a.m.	21.2164
21	-74.94376814	11.03626373	23/09/2008	11:00:00 a.m.	17.2349
23	-74.97002218	10.99460634	23/09/2008	12:00:00 p.m.	11.5726
25	-74.86193217	11.09966182	24/09/2008	9:45:00 a.m.	34.7015
28	-74.88173425	11.08059369	24/09/2008	12:36:00 p.m.	16.9597
27	-74.87537733	11.08711313	24/09/2008	12:16:00 p.m.	13.8642
29	-74.88579985	11.0884025	24/09/2008	1:05:00 p.m.	22.8866
30	-74.8859843	11.08789927	24/09/2008	1:40:00 p.m.	29.8175
31	-74.88036884	11.09623642	24/09/2008	2:03:00 p.m.	35.2936
32	-74.87481519	11.1027323	24/09/2008	2:22:00 p.m.	38.8291
35	-75.74406231	10.2510081	25/09/2008	12:30:00 p.m.	14.4672
36	-75.75141359	10.25710906	25/09/2008	12:47:00 p.m.	17.0092
38	-75.7643144	10.26960822	25/09/2008	1:25:00 p.m.	25.2684
40	-75.77655926	10.28179811	25/09/2008	2:10:00 p.m.	35.5999
42	-75.78847173	10.29435105	25/09/2008	2:50:00 p.m.	45.1205
43	-75.7951204	10.30047852	25/09/2008	3:10:00 p.m.	49.9387

Relative errors

SPM($a440$) Est.	SPM Meas.	Relative error (%)	Error
22.036	12.800	-72.158	85.307
14.966	9.800	-52.717	26.691
12.843	6.000	-114.046	46.823
32.943	24.600	-33.915	69.608
12.514	11.200	-11.729	1.726
MAE	46.031	**Mean relative error (%)**	-56.913
RSME	6.785	**Correlation**	0.942

SPM(b_b555) Est.	SPM Meas.	Relative error (%)	Error
15.237	12.800	-19.039	5.939
18.008	9.800	-83.757	67.374
13.985	6.000	-133.076	63.754
25.546	24.600	-3.846	0.895
11.937	11.200	-6.583	0.544
MAE	27.701	**Mean relative error (%)**	-49.260
RSME	5.263	**Correlation**	0.852

Appendix E. Complete results of Wavelet Analysis

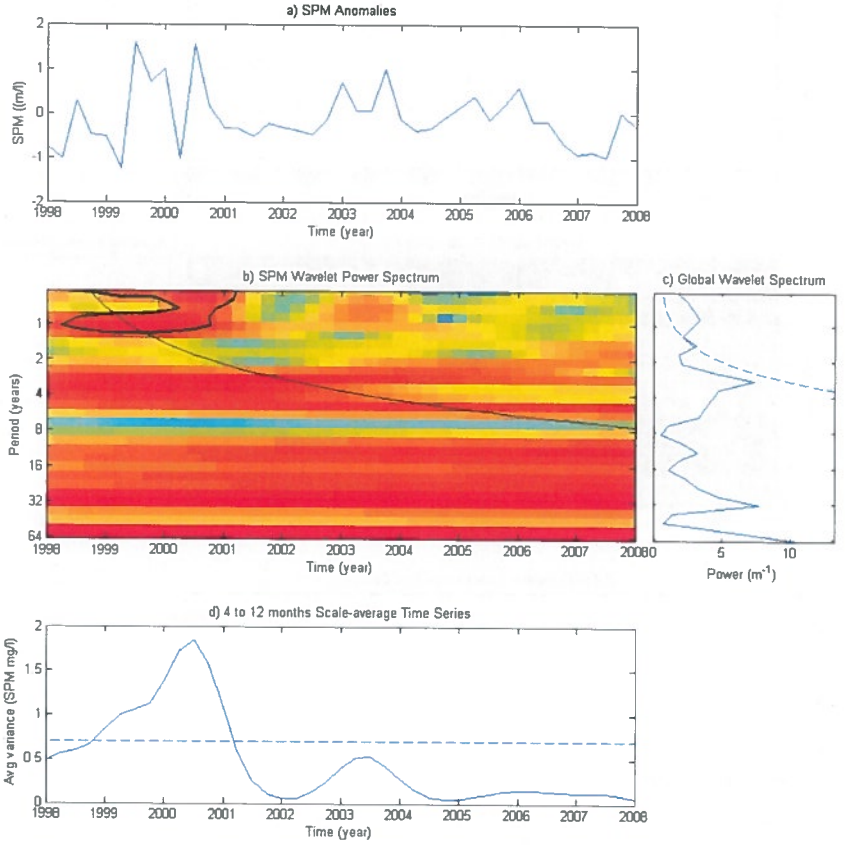

SPM wavelets analysis 1998-2008, Rosario Islands

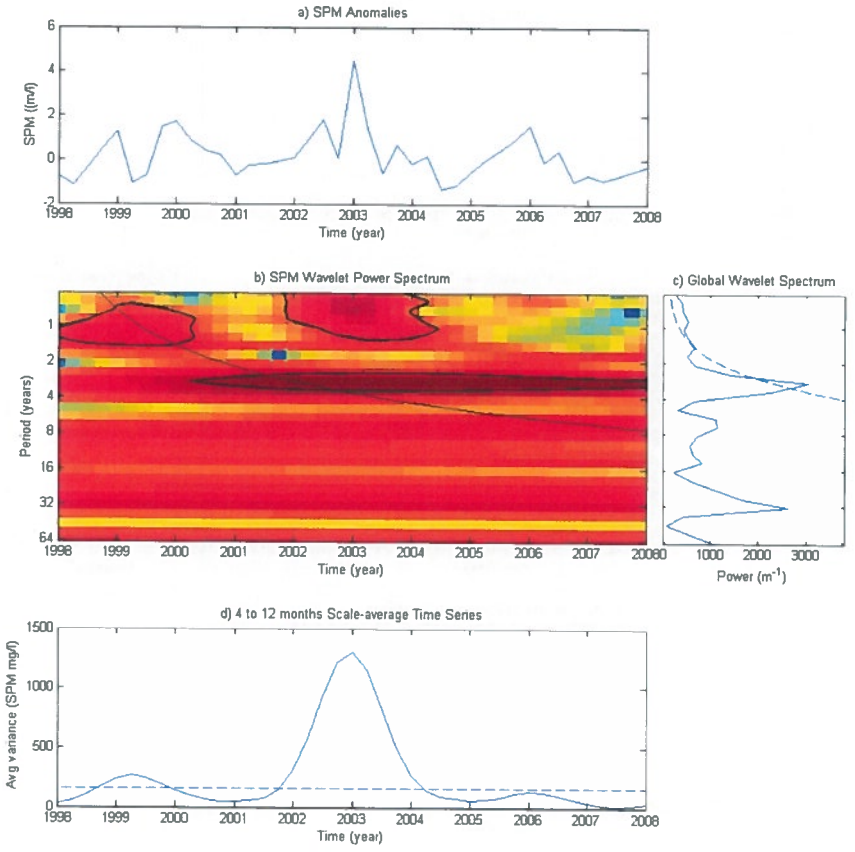

SPM wavelets analysis 1998-2008, Magdalena River mouth

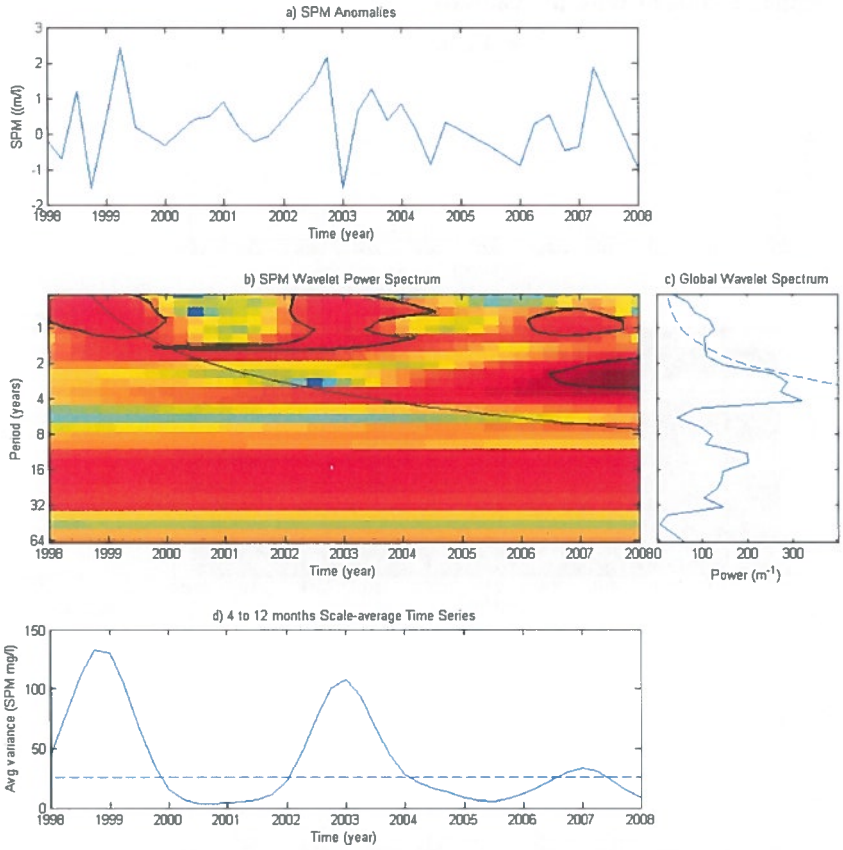

SPM wavelets analysis 1998-2008, Magdalena River mouth

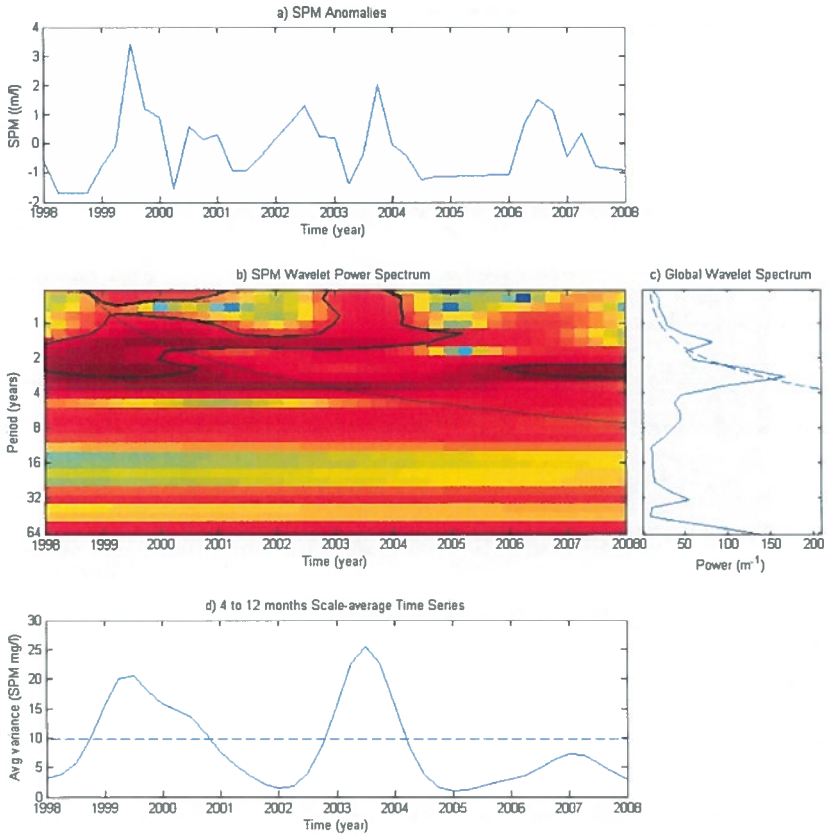

SPM wavelets analysis 1998-2008, Sinú River mouth